Spring 2014

Studies of influencing factors for shale gas reservoir performance

Jiaqi Wang

STUDIES OF INFLUENCING FACTORS FOR SHALE GAS RESERVOIR PERFORMANCE

by

JIAQI WANG

A THESIS

Presented to the Faculty of the Graduate School of the

MISSOURI UNIVERSITY OF SCIENCE AND TECHNOLOGY

In Partial Fulfillment of the Requirements for the Degree

MASTER OF SCIENCE IN PETROLEUM ENGINEERING

2014

Approved by

Dr. Mingzhen Wei, Advisor
Dr. Baojun Bai
Dr. Shari Dunn-Norman

ABSTRACT

Shale gas resource plays a significant role in energy supply worldwide. For economic production of shale gas, technologies of horizontal well and hydraulic fracturing are used for shale gas reservoirs. Therefore, the productivity of the shale gas reservoirs will be influenced by both reservoir condition, and hydraulic fracture properties.

In this thesis, parameters that will influence shale gas production were classified into two categories: reservoir properties and hydraulic fracture properties. Published shale gas simulation studies were surveyed for determining the typical ranges of those properties. CMG-GEM was employed to finish the reservoir simulation work, and CMG-CMOST was used to complete the sensitivity analysis work.

A three dimensional single phase dual-permeability shale gas reservoir model was created. Three flow mechanisms (Darcy flow, Non-Darcy flow, and Gas diffusion) as well as gas adsorption and desorption mechanism were considered in this model.

Sensitivity checks for each parameter were performed to analyze the effect of factors to forecast the production of shale gas reservoir. Influences of reservoir and hydraulic fracture parameters for different time periods were quantified by simulation of 1 yr., 5 yr., 10 yr., and 20 yr. production

ACKNOWLEDGMENTS

Foremost, I would like to express my sincere gratitude to my advisor Prof. Mingzhen Wei for the continuous support of my Master study and research, for her patience, motivation, enthusiasm, and immense knowledge. Her guidance helped me throughout my research and writing of this thesis. I could not have imagined having a better advisor and mentor for my Master study.

Besides my advisor, I would like to thank the rest of my thesis committee: Prof. Baojun Bai and Prof. Shari Dunn-Norman, for their encouragement, insightful comments, and hard questions.

Also, I would like to thank Thanh Nguyen and Nosser Jurado from CMG support team for their patient explanations of application of CMG software.

Last but not the least, I would like to thank my family: my parents Shijian Wang and Xingfen Xu, for giving birth to me at the first place and supporting me spiritually throughout my life.

TABLE OF CONTENTS

Page

LIST OF ILLUSTRATIONS

Page

LIST OF TABLES

Page

NOMENCLATURE

Symbol	Description
K_n	Knudsen number
V_L	Gas Langmuir volume, SCF/ton
P_L	Gas Langmuir pressure, psi
P_g	In-situ gas pressure in the pore system, psi
Area	The contact area between blocks i and j
Separation	The distance between blocks i and j (computed from the fracture spacings)
diffuse (k)	Diffusion coefficients (cm2/sec) for the hydrocarbon components
tortuo	A positive real number giving the tortuosity of the porous medium
phi	The porosity of the matrix block
Sg	The smaller of the gas saturations in blocks i and j
C(k,gas,i)	The concentration of component k in the gas phase of block i (moles per unit volume of the gas phase)
C(k,gas,j)	The same for block j
β	Forchheimer factor
k_{app}	Apparent permeability.
k	Permeability of porous media
p	Reservoir pressure
μ	Gas viscosity
ρ	Gas density
MPOR	Matrix porosity, friction
CPOR	Rock compressibility, 1/psi

NFPOR	Natural fracture porosity, friction
MPERM	Matrix permeability, md
LangV	Langmuir volume, gmole/lb
LangP	Langmuir pressure, 1/psi
SPACING	Hydraulic fracture spacing, ft
HALFLENGTH	Hydraulic fracture half-length, ft
HEIGHT	Hydraulic fracture height, ft
CONDUCTIVITY	Hydraulic fracture conductivity, ft

1. INTRODUCTION

1.1. SHALE GAS

Shale gas is a kind of natural gas produced from gas shale which is both source rock and storage reservoir. In the shale gas reservoir, gas is presented as two states: free gas in the porous media and adsorbed gas on the surface of organic material. As shale has extremely low permeability which is about 10 to 100 nano-Darcy, economically development of shale had been regarded as impossible for a very long time.

In 1998, Mitchell Energy finished the first economical shale gas fracturing work by using slick-water fracturing method. After that, shale gas gradually becomes an important part of natural gas production.

From 2005 to 2013, shale gas had experienced a rapid growth which is mainly caused by two technologies. The first one is hydraulic fracture technology. Compared with conventional natural gas reservoirs, shale gas reservoirs have extremely low permeability and porosity which make it almost impossible to achieve economic production, if just rely on traditional developing methods. The application of fracturing technology can effectively solve the problem by producing hydraulic fractures. The second one is horizontal well technology. Even though the low permeability problem has been solved by the hydraulic fracture technology, the limited stimulated volume of vertical wells still constrains the development of shale gas reservoirs. A horizontal well which is drilled to intersect the pay zone can extremely increase the contact area of wellbore and thus increase the stimulated volume. The combination of horizontal well drilling and hydraulic fracturing technology can significantly improve both the reservoir permeability and the stimulated volume.

1.2. SHALE GAS RESERVOIR IN THE UNITED STATES

It has been nearly 200 years since the first shale gas well was drilled in Fredonia, New York. However, only in last few decades large scale of shale gas development has been started.

According to the prediction made by U.S. Energy Information Administration (EIA) (Figure 1.1 and Figure 1.2), from 2011 to 2040, the total natural gas production in U.S. will increase from 23.0 trillion cubic feet to 33.1 trillion cubic feet which will contribute 38% of the total energy production, as shown in Figure 1.1. And almost all of this increase is due to projected growth in shale gas production which grows from 7.8 trillion cubic feet in 2011 to 16.7 trillion cubic feet in 2040, as shown in Figure 1.2.

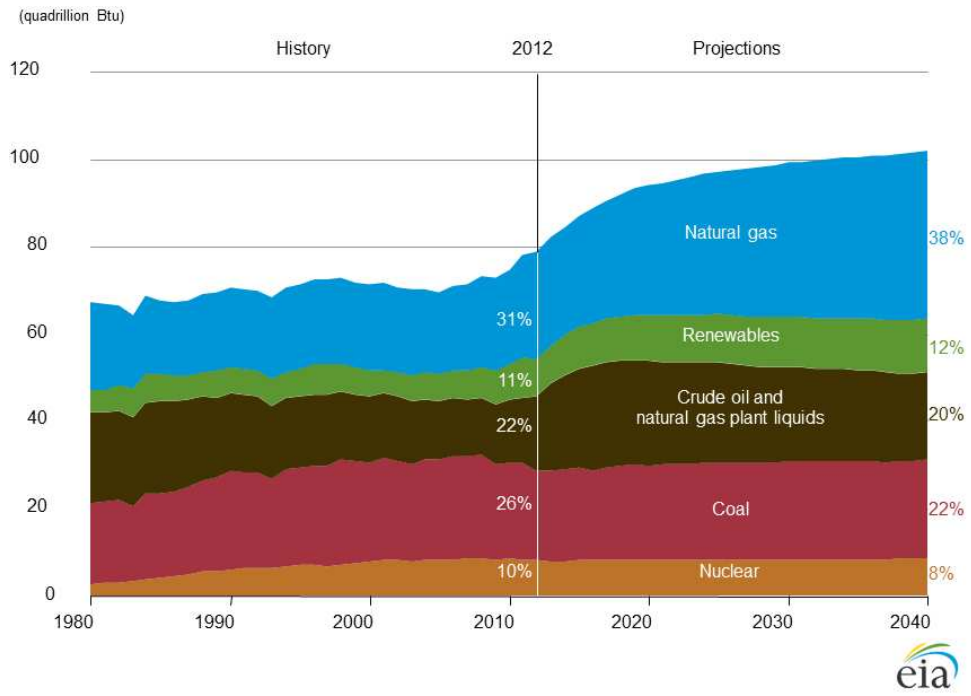

Figure 1.1 U.S. Energy Production by Fuel, 1980-2040 (EIA, 2013)

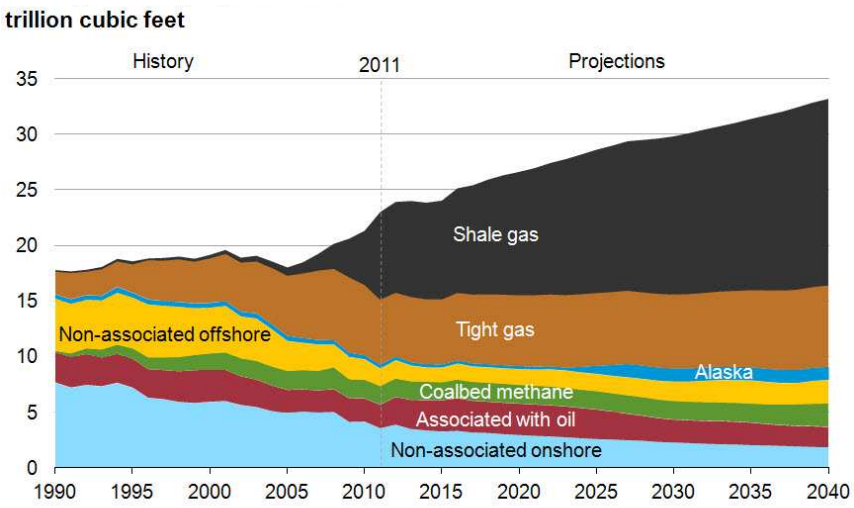

Figure 1.2 U.S. Dry Natural Gas Production (EIA, 2013)

In the lower 48 state of U.S., shale gas production is concentrated mainly in five important shale gas reservoirs: Barnett, Woodford, Fayetteville, Marcellus, and Haynesville as shown in Figure 1.3. Barnett Shale is one of the most successful shale gas reservoir and also is the first one that can economically produce gas from shales.

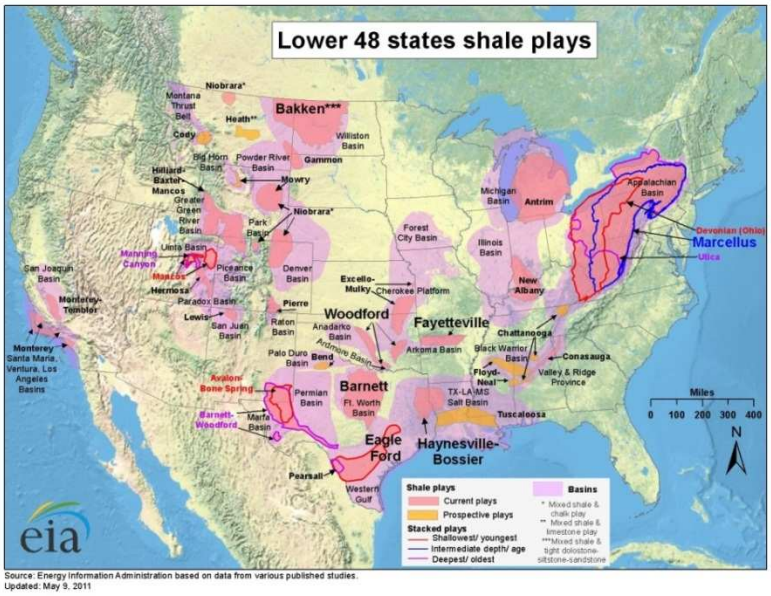

Figure 1.3 Shale Plays in Lower 48 States (EIA, 2011)

1.3. SHALE GAS DISTRIBUTION IN THE WORLD

According to the estimate made by EIA, the total amount of technically recoverable shale gas in the world is 7,299 trillion cubic feet. Table 1.1 gives the amount of technically recoverable shale gas of top 10 countries. Proven natural gas reserves of all types refer to amount of proved natural gas, including all conventional and unconventional natural gas. As shown in Table 1.1 for all countries, except Russia, amount of estimated technically recoverable shale gas is higher than proven natural gas reserves which mean the potential of shale gas is enormous.

Table 1.1 Shale Gas in the World (EIA, 2013)

	Country	Estimated technically recoverable shale gas (trillion cubic feet)	Proven natural gas reserves of all types (trillion cubic feet)
1	China	1,115	124
2	Argentina	802	12
3	Algeria	707	159
4	United States	665	318
5	Canada	573	68
6	Mexico	545	17
7	South Africa	485	-
8	Australia	437	43
9	Russia	285	1,688
10	Brazil	245	14

2. LITERATURE REVIEW

As a tool used to study and understand performance of reservoir, reservoir simulation has been widely used all over the world for more than 40 years. Compare with conventional reservoirs, shale gas reservoir simulation needs special features to deal with natural fractures, extremely low permeability, hydraulic fractures and gas adsorption on rock surface.

The goal of this research study is to build a shale gas reservoir simulation model that can be employed to do sensitivity analysis for factors which will influence well performance.

2.1. RESERVOIR SIMULATION MODELS FOR GAS SHALES

2.1.1. Single Porosity Model. In a single porosity model, the reservoir is discretized and fractures are represented explicitly with grid cells as single planar planes or network of planar planes (Li et al.2011).

Very finely gridded, single porosity model can present reliable result and usually has been used as reference model to check the accuracy of other model. However, this fine gridded model will need very long computational time which means it cannot be used widely (Cipolla et al. 2009).

2.1.2. Dual-Porosity Model. Dual-porosity model, developed by Warren and Root at 1963, is widely used in modeling hydraulically fractured shale gas reservoir.

In the classic dual-porosity reservoir model, the reservoir is composed of matrix and fracture (Figure 2.1). Compared with the single-porosity reservoir where gas directly flows from reservoir to well, in dual-porosity reservoirs gas flows through the fracture

network to the well. On the other hand, the fracture network is constantly recharged by flow from the matrix in the dual-porosity model (Carlson, E.S. and Mercer, J.C. 1991).

The matrix system which occupies most volume of the model represents the storage of free gas and adsorbed gas. The fracture system which only occupies a small part of the whole model has relatively high permeability and is the mainly path for gas flow.

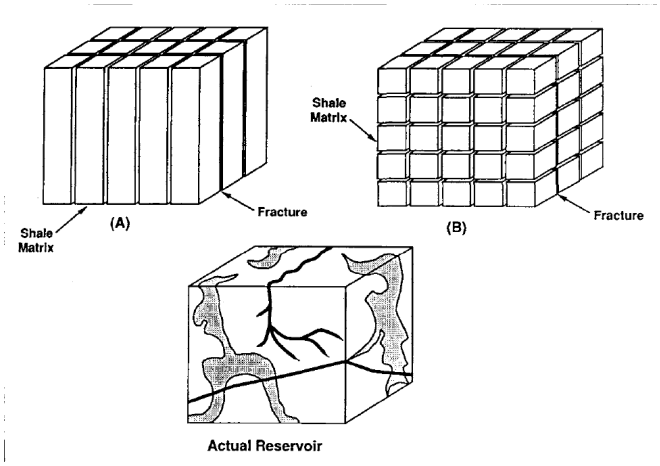

Figure 2.1 Explanation of Dual-porosity Model (Carlson et al. 1991)

As most shale gas reservoirs are naturally fractured reservoir, dual-porosity model is very popular in the field of shale gas reservoir simulation. A lot of studies have been done on this area.

Du et al. (2010) simulated the hydraulically fractured shale gas reservoir as a dual porosity system. Microseismic responses, hydraulic fracturing treatments data and production history-matching analysis were applied to finish the analysis. Proppant distribution and fracture conductivity were discussed. They also did sensitivity studies for

parameters including rock mechanical and stress data, water holdings in fracture network, fracture network conductivity, and micro-seismic intensity.

Zhang et al. (2009) built up a dual-porosity simulation model to analyze the influence of different parameters to the simulation of a single horizontal well. Their dual-porosity model was developed by upscaling the discrete fracture network (DFN) model. Thirteen different parameters were tested to analyze their impact on cumulative gas production. This work was completed by using ECLIPSE (Reservoir simulator by Schlumberger).

Li et al. (2011) compared Single porosity and Dual porosity modeling methods and presented their similarities and differences. In their study, both single and dual porosity system can receive the similar result of production response. Li et al. also pointed out that although the model seems matching the history data, for a shale gas reservoir which only has a short history data may not able to give a reasonable prediction of the future performance. However, for achieving the same accuracy of result, single porosity model created five times more grids than dual-porosity model, which means this single porosity case will cost much more time.

2.1.3. MINC (Multiple Interaction Continua Method). The Multiple Interaction Continua Method (MINC) method, developed by Pruess and Narasimhan (1985), is an extension of dual-porosity approach. Similar with the dual-porosity model, in MINC modeling, the fractured reservoir will be firstly divided into gridblocks; and then each of these gridblocks is composed of two porosity systems: fracture porosity and matrix porosity. After that the matrix part in MINC method will be subdivided into a

sequence of nested rings which will make it possible to calculate the interblock fluid flow by calculating flow between rings, as shown in Figure 2.2.

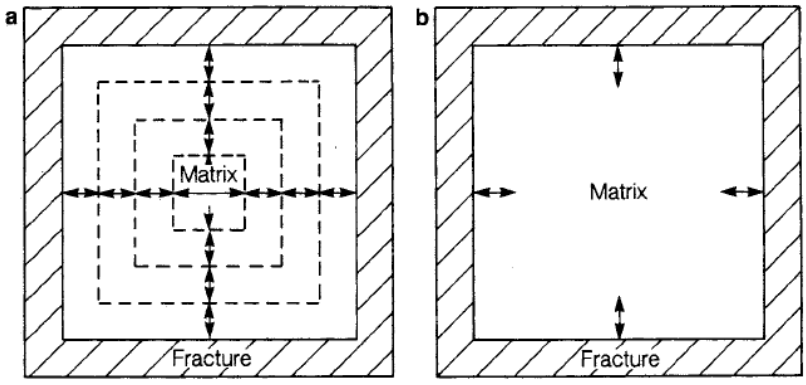

Figure 2.2 Discretization of Matrix Blocks: a. MINC, b. Dual-porosity model (Yu-Shu Wu et al. 1988)

2.1.4. Dual Permeability Model. Same with the classical dual-porosity model, in the dual permeability model, the reservoir is assumed to consist of matrix and fractures system. Each of them has their own properties, such as porosity, permeability, water saturation, etc. So, each grid has one matrix porosity and one fracture porosity.

As shown in Figure 2.3, for the flow inside each grid, both matrix to matrix flow and matrix to fracture flow will be considered. And the matrix properties will dominate the matrix to fracture flow. For the flow between grids, different from the traditional dual-porosity model, the matrix porosities in the dual permeability model is also connected with neighboring matrix porosities, like fracture porosities.

Moridis (2010) built up a dual permeability model and compared it with the dual porosity model and the Effective Continuum Model (ECM). At the same time, they created a reference case with extremely fine domain discretization, complex descriptions

of the fracture-matrix interactions in several subdomains of the producing system, and assuming that this reference case is reliable enough to evaluate the suitability of simplified approaches. Their results showed that dual permeability model offered the best performance of the three models evaluated. But they also pointed out that, during the later time of production, the deviations between reference case and dual-permeability case become more obvious.

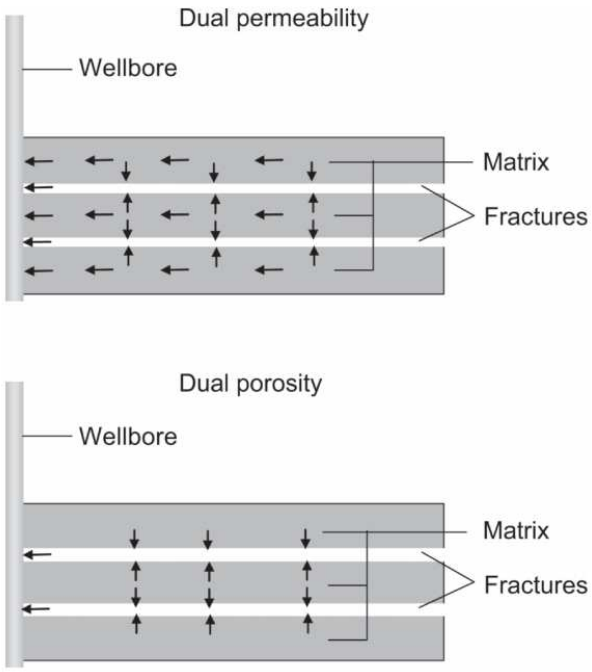

Figure 2.3 Illustration of Flow in Dual Porosity Model and Dual Permeability Model (Pereira et al. 2006)

2.1.5. Multiple Porosity Model. Compared with the dual-porosity model which assumes that the reservoir is made up of matrix and fracture two parts, in the multi-porosity model, the matrix is further separated into two or three parts based on different properties, such as pore size and rock type(organic or inorganic).

Dehghanpour et al. (2011) further assumed that the matrix blocks in the dual porosity model is composed of sub-matrices with nano Darcy permeability pores and micro fractures with milli to micro Darcy permeability. The result of sensitivity analysis shows that by taking micro fractures into the consideration, the rate of wellbore pressure drop has been significantly decreased.

Yan et al. (2012) presented a micro-scale model. In this model, the shale matrix bulk was further separated into inorganic matrix and organic matrix, and the organic part was further divided into two parts basing on pore size on kerogen: organic matter with vugs and organic matter with nanopores. Therefore there are four different continua in their model: nano organic matrix, vugs organic matrix, inorganic matrix and fracture. Compared with the conventional dual-porosity model, in micro-scale model, system is more producible and the pressure drop is much faster. They also built up a triple permeability model in which all fractures, inorganic and organic porosity systems are allowed to flow among themselves and between different porosity types.

2.2. GAS DESORPTION

Gas desorption is an important aspect of shale gas study. The well know adsorption isotherm which shows the relationship between volume of gas adsorbed and pressure at constant temperature is widely used in gas desorption/adsorption analysis.

It is accepted by everyone that gas desorption mechanism has great impact on shale gas production, but on earth to what degree that gas desorption will influence the well performance and its impact on economics are still controversial.

Bumb et al. (1998) developed an approximate analytic solution for gas flow in gas reservoirs where both free gas and adsorbed gas exist. Then this solution was

implemented to test the effect of gas desorption. The result shows that compared with conventional reservoir without adsorbed gas, a reservoir containing adsorbed gas will receive higher cumulative production.

Cipolla et al. (2009) analyzed the impact of gas desorption by doing simulation study using real reservoir data from Barnett and Marcellus Shales. They found that for Barnett Shale the impacts of gas desorption is mainly occurring in the late life of the well when matrix pressure become low, an increase of 5%-15% in 30-year gas recover has been predicted. Marcellus shale reservoir shows similar trend with Barnett, and presents a 10% increase in 30-year production. And they concluded that gas desorption may not give significant impact on economics.

Moridis et al. (2010) used the muti-component Langmuir isotherm equation to analyze the effect of the amount of sorbed gas on gas production. They changed the Langmuir Volume to 0, 100, and 200 scf/ton. The result shows that the amount of sorbed gas has significant impact on the prediction of production.

Yu et al. (2013) observed that gas desorption contributes over 20% of increase in EUR at 30 years of gas production for New Albany Shale and Marcellus Shale; below 10% increase in EUR for Haynesville Shale; between 10% and 20% increase in EUR for Barnett Shale and Eagleford Shale. They also pointed out that the gas desorption is more important when fracture spacing is decreasing.

2.3. FLOW MECHANISMS IN GAS SHALES

In a shale gas reservoir, the scales of pore radius are in large variations. On one hand, hydraulic fractures have macro scale pores; on another hand, the pores in the matrix

are in Nano-scale. This giant variation of pores scale makes the flow of gas in shale reservoir become very complexity.

Javadpour et al. (2007) described the flow in nanopores as either the continuum or the molecular approach and described different flow regimes basing on Knudsen number. They built up an approach for describing gas flow in nanopores. Table 2.1 describes different flow regimes basing on the Knudsen number.

Table 2.1 Flow Regimes Based on Knudsen Number (Javadpour et al. 2007)

Navier-Stokes Equation	
No-slip ($K_n < 0.001$)	Slip ($0.001 < K_n < 0.1$)
Continuum flow	Slip flow
Darcy flow	Knudsen Diffusion

Freeman et al. (2010) described the gas flow in shales as three separate mechanisms: convective flow, Knudsen diffusion, and molecular diffusion. They applied the Klinkerberg's method to solve the Knudsen diffusion, and the Chapman-Enskodd model to estimate molecular diffusion.

Swami et al. (2012) further identified four flow regimes in shale gas reservoirs as based on Knudsen number: Viscous flow (≤ 0.001), Slip flow ($0.001<K_n<10$), Transition flow ($0.1<K_n<10$), and Knudsen's flow ($K_n \geq 10$). They summarized and compared 10 different theories used for calculating the non-Darcy flow, and concluded that Javadpour's model is the most reasonable approach, but still needs validation against real field data.

3. MODEL SELECTION IN SIMULATION GAS FLOW IN SHALES

3.1. RESERVOIR MODEL

In this study, a Dual-permeability model has been proposed for constructing reservoir simulation model for shale gas simulation. Same with the classical Dual-porosity model, in this model, the shale gas reservoir is assumed to consist of matrix and fractures. Each of them has their own properties, such as porosity, permeability, water saturation, etc. Therefore, each grid has one matrix porosity and one fracture porosity.

For the flow inside the grid, both matrix to matrix flow and matrix to fracture flow will be considered. The matrix properties will dominate the matrix to fracture flow. For the flow between grids, different from the traditional dual-porosity model, in which matrix is only connected with fracture in the same grid, the matrix porosities in the dual-porosity dual permeability model is also connected with neighboring matrix porosities. That means not only fracture is connected with fracture in other grids, matrix also is connected with matrix in other grids. Figure 3.1 shows the explanation of flow in dual-permeability model.

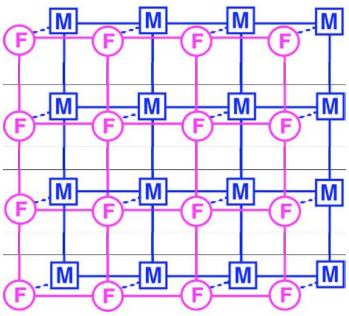

Figure 3.1 Flow Connections in the “dual permeability” Model. Global flow occurs between both fracture (F) and matrix (M) grid blocks. In addition there is F-M interporosity flow (Pruess et al., 1999).

3.2. GAS DESORPTION

For the gas adsorption/desorption phenomenon, the Langmuir isotherm is the most popular model. By using the Langmuir equation (Langmuir, 1918), the amount of gas adsorbed on the rock surface can be computed.

$$\mathrm{C}(P_g) = V_L \frac{P_g}{P_g + P_L} \tag{1}$$

V_L—gas Langmuir volume, SCF/ton

P_L—gas Langmuir pressure, psi

P_g—in-situ gas pressure in the pore system, psi

In this equation, Langmuir volume means the maximum amount of gas that can be adsorbed on the rock surface under infinite pressure. Langmuir pressure is the pressure when the amount of gas adsorbed is half of the Langmuir volume. These two parameters play important roles in the gas desorption process. For different shale gas reservoir, the contrasts of Langmuir volume and Langmuir pressure lead to distinct trend of gas content. Table 3.1 gives the Langmuir parameters data of five main shale gas reservoirs in the US. Figure 3.2 shows the relationship between adsorption gas content and reservoir pressure.

From Figure 3.2, it is clear that Langmuir volume determine the amount of gas that can be adsorbed in high pressure condition, and Langmuir pressure determine how the decline of gas content corresponds to the decline of pressure.

Table 3.1 Langmuir Parameters Data of Five Major Shale Gas Reservoirs in the U.S. (Wei et al. 2013).

	Barnett	Marcellus	Eagleford	Haynesville	New Albany
Langmuir pressure (psi)	650	500	1500	1500	412.5
Langmuir volume (SCF/ton)	96	200	175	60	104.2

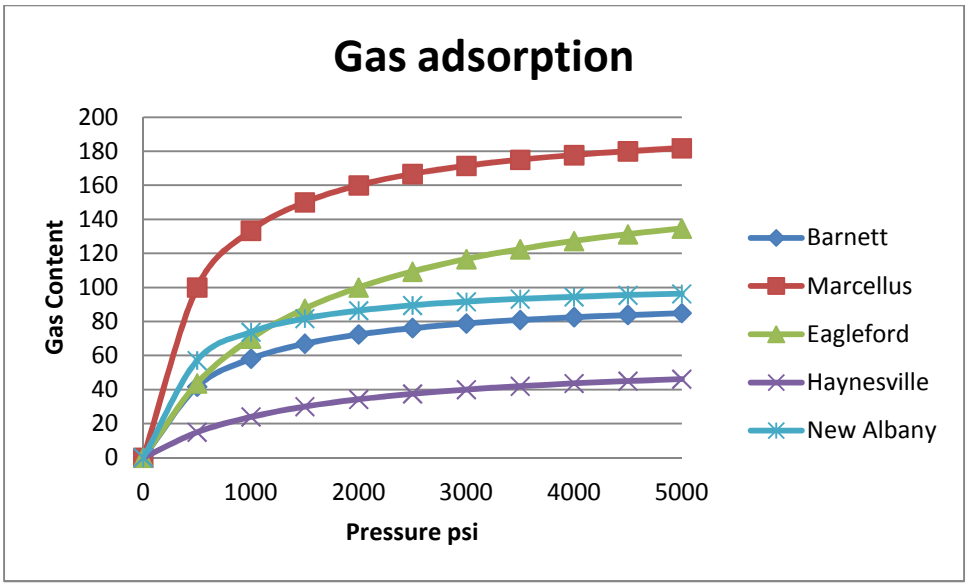

Figure 3.2 Langmuir Isotherm Curve for Five Shale Gas Reservoirs

3.3. FLOW MECHANISM

Due to the complexity of flow in shale gas reservoir, three kinds of flow mechanisms are applied in our dual-permeability model: Darcy flow in natural fractures, gas diffusion in nano pores in matrix and Forchheimer flow in hydraulic fractures.

3.3.1. Gas Diffusion. Compared with conventional gas reservoir, shale gas reservoir has extremely low permeability; and the pore size of shale is between 1 to 200 nanometers (Swami et al. 2012).

The gas flow in macro-scale pores, such as hydraulic fractures and natural fractures, is following the Darcy's law and can be applied as same as the conventional reservoir. But the gas flow in the nano-scale pores will no longer follow the Darcy's law. For this part of the reservoir, diffusion flow should be considered. Figure 3.3 presents the classification of flow type basing on permeability, porosity, and r_{p35} pore throat values.

Hinkley et al. (2013) pointed out that Langmuir desorption actually occurs on the wall of pores. But gas cannot be transport to pores wall immediately; another theory is needed to calculate the gas diffuse from bulk body to pores wall.

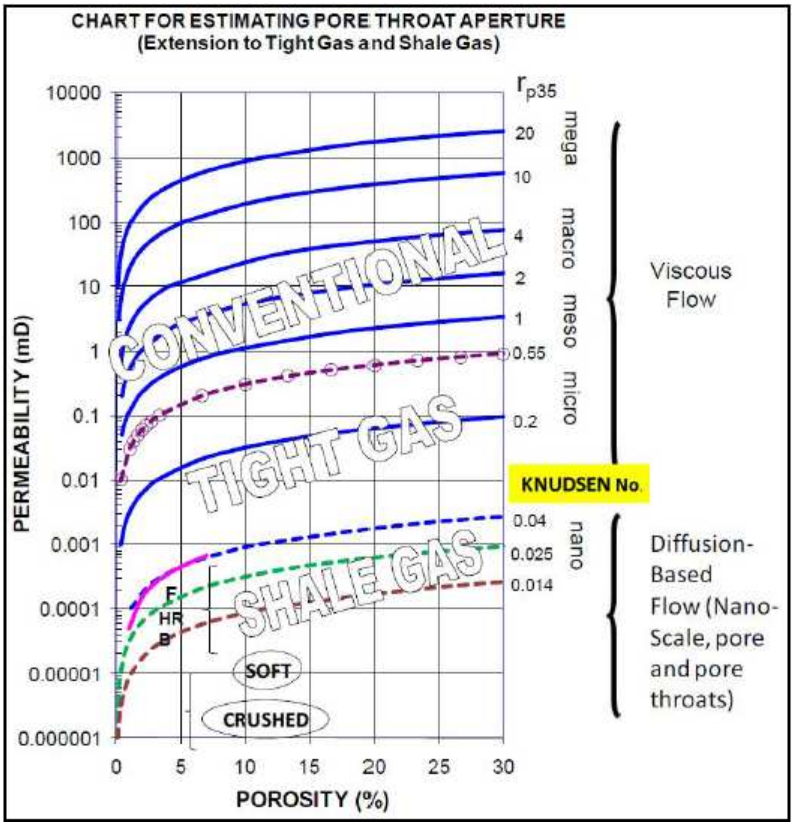

Figure 3.3 Integrated Crossplot of Porosity vs. Permeability (showing flow units for conventional, tight gas and shale gas reservoir based on r_{p35} pore throat values) (Rahmanian et al., 2010)

In CMG-GEM, the gas diffusion is presented by below equation:

$$V= (Area/L_{ij}) * (K_{diffuse}/T) * phi * Sg * (C(k, gas, i) – C(gas, j)) \quad (2)$$

V—The gas phase diffusion rate

Area—the contact area between blocks i and j,

L_{ij}—the distance between blocks i and j (computed from the fracture spacings),

$K_{diffuse}$ —diffusion coefficients (cm^2/sec) for the hydrocarbon components,

T—a positive real number giving the tortuosity of the porous medium,

phi—the porosity of the matrix block,

Sg—the smaller of the gas saturations in blocks i and j,

C(k,gas,i) —the concentration of component k in the gas phase of block i (moles per unit volume of the gas phase),

C(k,gas,j) —the concentration of component k in the gas phase of block j.

3.3.2. Forchheimer Flow in Hydraulic Fracture. At high flow velocities in the fractures, the relationship between pressure gradient and fluid velocity is no longer linear, so linear Darcy's flow is no longer valid. Gas flow in hydraulic fracture follows Forchheimer flow model **(**Moridis et al. 2010). Darcy's law describes the laminar flow regime with zero inertia whereas the Forchheimer equation represents the laminar flow regime with inertia effect.

Forchheimer Equation (H. Huang et al. 2006):

$$-\frac{\partial p}{\partial x} = \frac{\mu}{k}V + \beta\rho V^2 \tag{3}$$

k is permeability of porous media. Factor β is deduced experimentally from the slope of the plot of the inverse of the apparent permeability $\frac{1}{k_{app}}$ vs. a dimensional pseudo Reynolds number$\frac{\rho V}{\mu}$.

$$\frac{1}{k_{app}} = -\frac{\partial p}{\partial x}\frac{1}{\mu V} = \frac{1}{k} + \beta\frac{\rho V}{\mu} \tag{4}$$

k_{app} is apparent permeability.

4. RESERVOIR SIMULATION BASE MODEL CONSTRUCTION AND SIMULATION RESULTS

In this study, a base case model is built up for shale gas reservoir simulation and sensitivity analysis. Simulation studies are performed by using CMG-GEM. Figure 4.1 and Figure 4.2 show 2D and 3D view of the reservoir model.

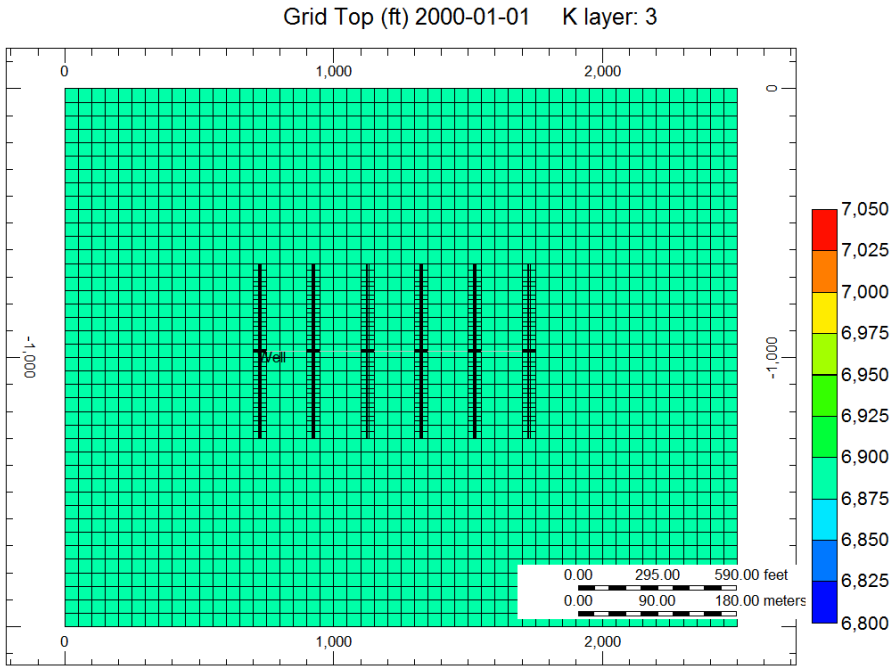

Figure 4.1 Reservoir Model with Hydraulic Fractures in the Middle of the Reservoir

The model dimension in areal is 2500 ft * 2000 ft. In Z direction, the model has 6 layers, and each of them is 50 ft in height (Figure 4.2). The top of first layer is 6800 ft. A horizontal well is drilled in the middle of the reservoir. Natural fractures are existed in this reservoir. The horizontal wellbore length is 1000 ft. Hydraulic fractures have been created. Table 4.1 gives the summary of reservoir parameters.

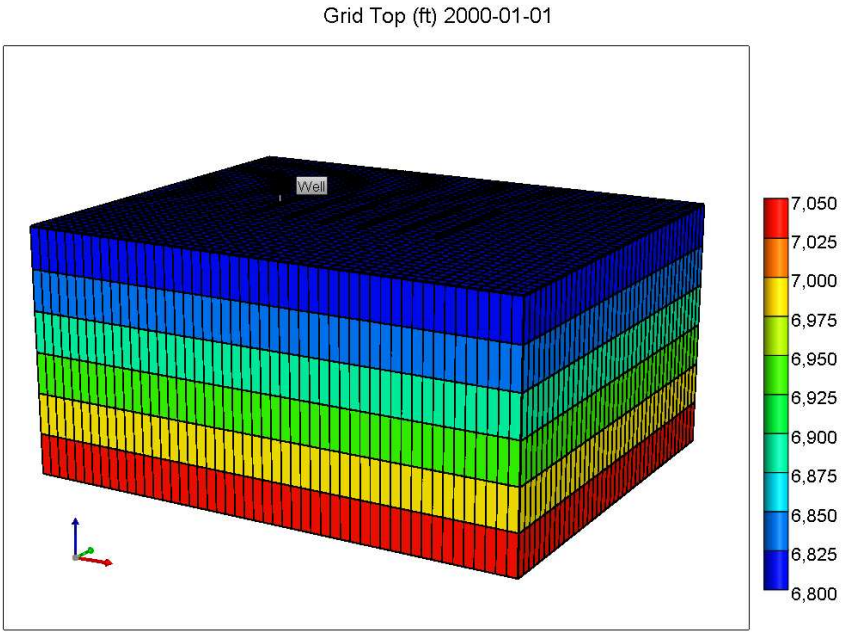

Figure 4.2 3D View of the Reservoir Model

Table 4.1 Summary of Base Case Value

Parameter	Value	Unit
Model Dimensions	2500*2000*300	ft
Initial Pressure	2400	psi
Depth	6800	ft
Average Temperature	200	°F
Bulk density	158	lb/ft3
Total Compressibility	3e-6	psi^{-1}
Langmuir Pressure	650	psia
Langmuir Volume	100	SCF/ton
Matrix Porosity	0.06	
Matrix Permeability	0.0002	mD
Natural Fracture Porosity	0.02	
Natural Fracture Permeability	0.01	mD
Hydraulic Fracture Conductivity	2	mD*ft
Hydraulic Fracture Spacing	200	ft

Table 4.1 Summary of Simulation Parameters (cont.)

Hydraulic Fracture Half-length	300	ft
Hydraulic Fracture Height	220	ft
Horizontal Well length	1000	ft
BHP	500	psi
Gas Diffusion	1e-08	m^2/s

Figure 4.3 and Figure 4.4 presents the result of production forecast for base case simulation. Both cumulative production and gas production rate for 20 years are showed.

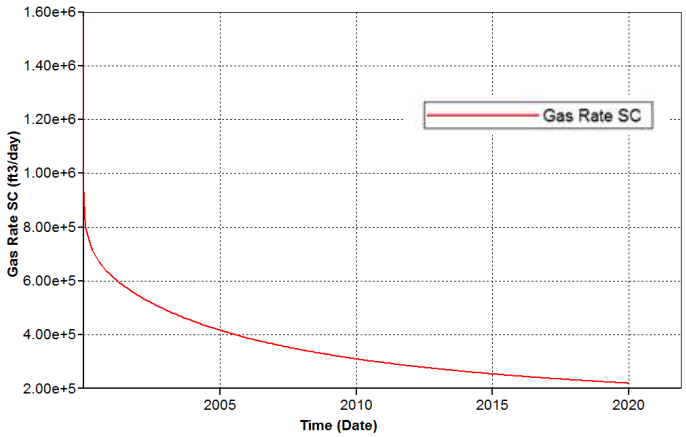

Figure 4.3 Simulation Result of Base Case for Gas Rate

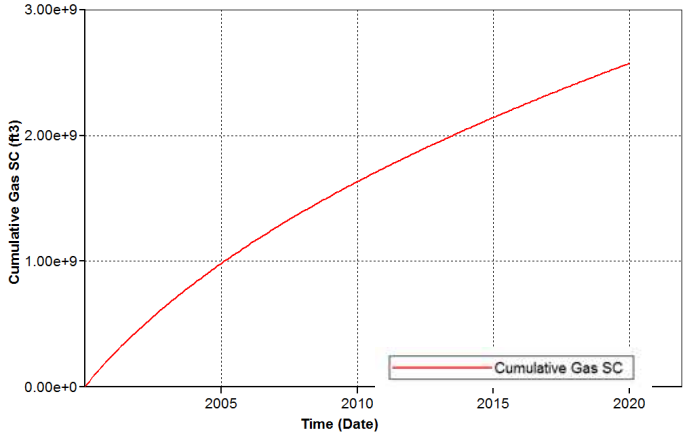

Figure 4.4 Simulation Result of Base Case for Cumulative Gas Production

Figure 4.5 and Figure 4.6 give the change of distribution of pressure from ten years to twenty years of Layer 3 in which the horizontal well is located. From these two figures, it is clear that, for both 10 years' simulation and 20 years' simulation, the range of pressure drop do not touch the boundary of reservoir.

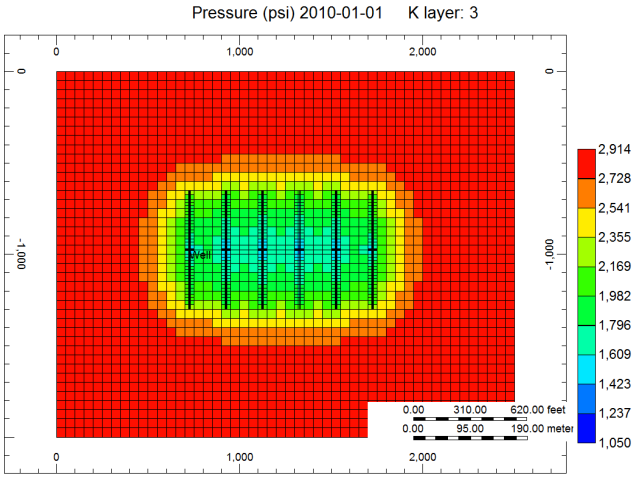

Figure 4.5 Pressure Distribution of Layer 3 after 10 Years Production

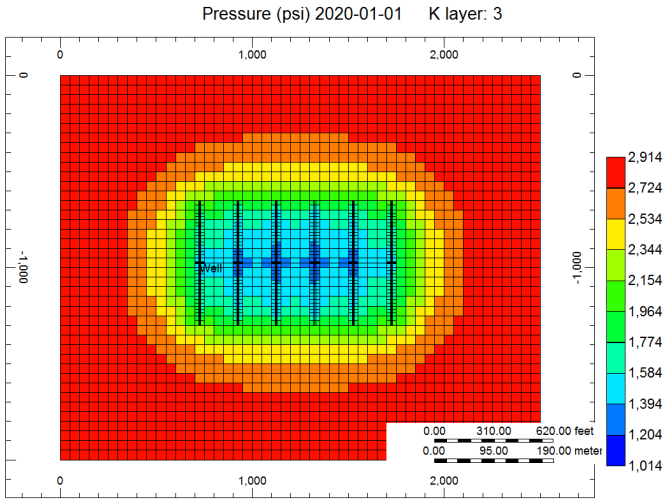

Figure 4.6 Pressure Distribution of Layer 3 after 20 Years Production

5. INFLUENCING FACTOR SENSITIVITY ANALYSIS

Sensitivity analysis of this thesis is constructed based on the base case and surveyed range of shale gas properties. In total of nine parameters has been considered during the analysis. As summarized in Table 5.1, these parameters are divided into two categories: a) reservoir parameters and b) hydraulic fracture parameters. Reservoir parameters include matrix porosity, matrix permeability, natural fracture porosity, Gas desorption (including Langmuir pressure and Langmuir Volume), and rock compressibility. Hydraulic fracture parameters include Hydraulic fracture conductivity, Hydraulic fracture spacing, hydraulic fracture half-length, and hydraulic fracture height.

Table 5.1 Classification of Major Parameters in the Simulation Model and their Ranges in Sensitivity Analysis

<table>
<tr><th colspan="2">Reservoir parameters</th><th>Range</th><th>Hydraulic Fracture parameters</th><th>Range</th></tr>
<tr><td colspan="2">Matrix Porosity</td><td>0.02 - 0.10</td><td>Hydraulic Fracture Conductivity (md-ft)</td><td>1 - 9</td></tr>
<tr><td colspan="2">Matrix permeability (md)</td><td>10^{-3} - 10^{-5}</td><td>Hydraulic Fracture Spacing (ft)</td><td>100 - 500</td></tr>
<tr><td colspan="2">Natural Fracture Porosity</td><td>0.005 - 0.04</td><td>Hydraulic Fracture Half-length (ft)</td><td>100 - 500</td></tr>
<tr><td rowspan="2">Gas Desorption</td><td>Langmuir Pressure (psi)</td><td>400 - 1500</td><td rowspan="2">Hydraulic Fracture Height (ft)</td><td rowspan="2">100 - 300</td></tr>
<tr><td>Langmuir Volume (SCF/ton)</td><td>60 - 220</td></tr>
<tr><td colspan="2">Rock compaction (psi^{-1})</td><td>10^{-4} - 10^{-6}</td><td></td><td></td></tr>
</table>

For determining range of sensitivity parameters, box plot is employed to summarize the data collected from different published papers. Box plot is a standardized way to present the distribution of data. The box plots used in this paper are based on five number summaries: the minimum, the first quartile, the median, the third quartile, and the maximum. Figure 5.1 presents the explanation of box plot used in this study.

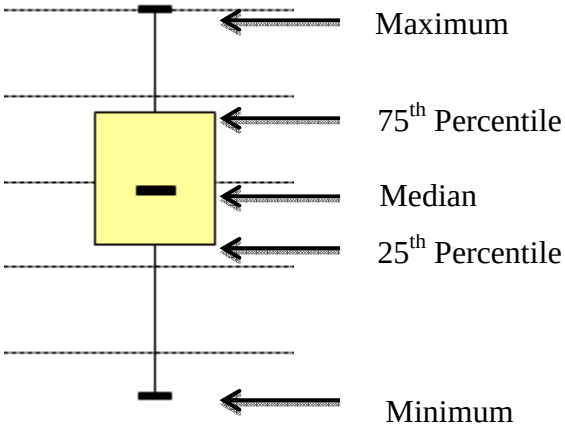

Figure 5.1 Box Plot – Explanation

Response surface methodology (RSM) is applied to explore the relationships between parameters and cumulative production. The main idea of RSM is to use a set of designed experiments to build a proxy (approximation) model to represent the original complicated reservoir simulation model (CMG-CMOST User's Guide – Version 2013). In this thesis, reduced quadratic proxy model is applied to estimate the effect of each parameter.

$$y = a_0 + \sum_{j=1}^{k} a_j x_j + \sum_{j=1}^{k} a_{jj} {x_j}^2 + \sum_{i<j} \sum_{j=1}^{k} a_{ij} x_i x_j \qquad (5)$$

In this proxy model, a_j, a_{jj}, and a_{ij}, are parameter estimate coefficients. Larger coefficient means the parameter is more important to the final result.

Tornado plot was applied to give a visual display of effect estimate results. In the tornado plot, the actual predicted response change as the parameter (or the cross term and quadratic) travels from the smallest sample value to the largest sample value was reported. The Maximum bar represents the maximum cumulative production among all the training jobs. The Minimum bar represents the minimum cumulative production among all the training jobs.

As there are too many combinations when analyzing the effect and interplay of a set of parameters, it will be impossible to cover all combinations in the experiment. Latin Hypercube sampling was used to generate job patterns from all possible job patterns. A job pattern represents the combination of one particular sample value for each parameter in the simulation model. Latin hypercube sampling (LHS) is a statistical method for generating a sample of plausible collections of parameter values from a multidimensional distribution. The sampling method is often used to construct computer experiments (CMG-CMOST User's Guide – Version 2013).

5.1. SENSITIVITY ANALYSIS OF RESERVOIR PARAMETERS

In this section, influence of each reservoir parameter will be studied separately. After that, all the parameters will be gathered together to analyze interplay between them. Parameters studied in this section include: matrix porosity, matrix permeability, natural fracture porosity, Langmuir pressure, Langmuir volume, and rock compaction.

5.1.1. Effect of the Matrix Porosity. Compared with the porosity in conventional natural gas reservoir, which can be as high as 48% (Michael D. Max2006),

the porosity of shale gas reservoir is usually between 2% to 15%. Figure 5.2 and Figure 5.3 gives the distribution of matrix porosity summarized from published papers.

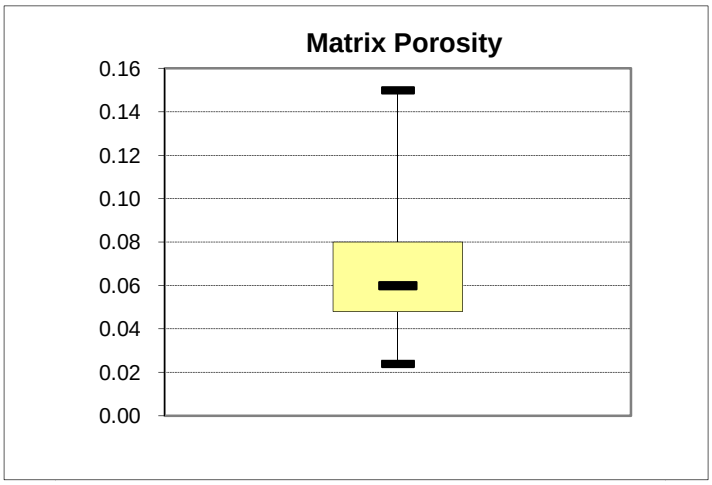

Figure 5.2 Box Plot of Matrix Porosity Data Collected

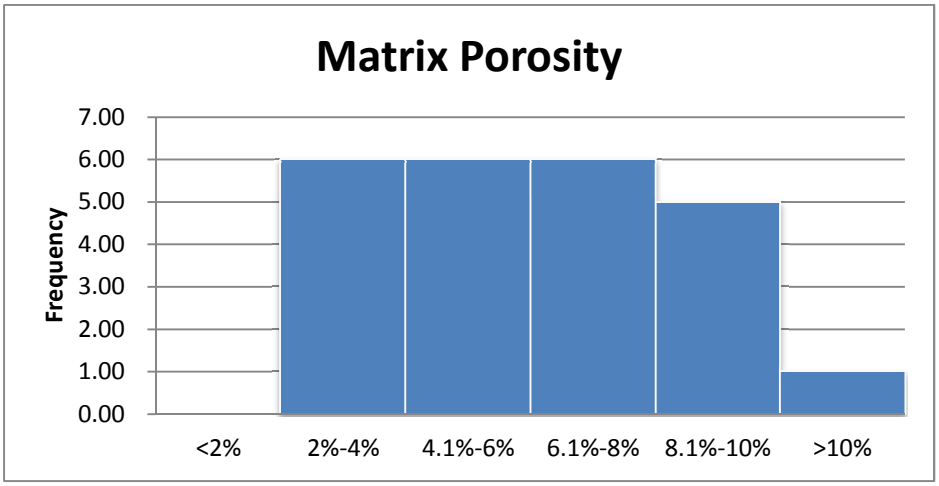

Figure 5.3 Histogram of Matrix Porosity Data Collected

Basing on the data collected from published papers, sensitivity analysis of matrix porosity to shale gas production was finished by using CMOST. Except Matrix porosity, all the other parameters applied in this simulation are same with base case model.

Influence of matrix porosity to cumulative production and gas rate are demonstrated in Figure 5.4 and Figure 5.5.

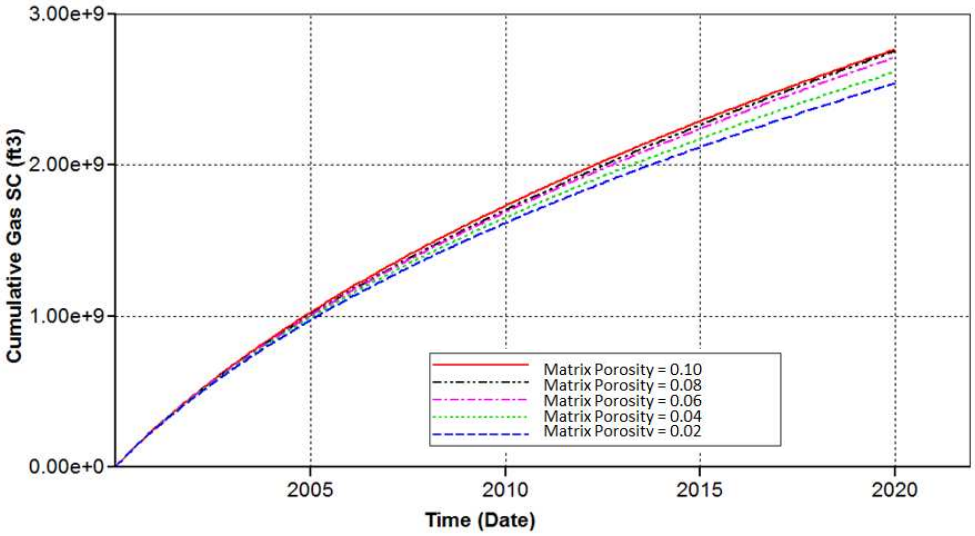

Figure 5.4 Impact of Matrix Porosity on Cumulative Production

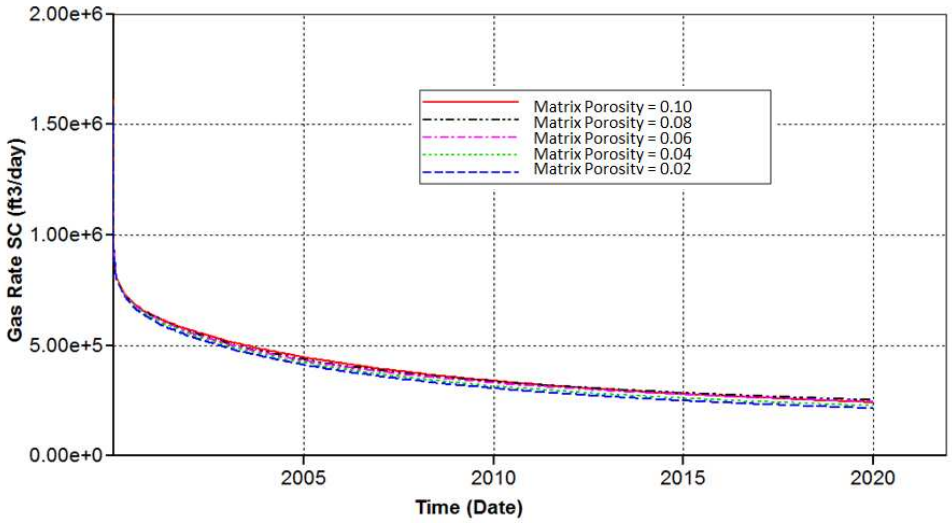

Figure 5.5 Impact of Matrix Porosity on Gas Rate

Figures 5.4 and 5.5 demonstrate the influence of matrix porosity on shale gas production. Basing on the simulation result, the 20 years cumulative production of

reservoir with 10% matrix porosity will be 2765 MMSCF, and the 20 years cumulative production of reservoir with 2% matrix porosity will be 2541 MMSCF. An 8.1% difference has been achieved between the lowest matrix porosity and the highest one.

5.1.2. Effect of the Matrix Permeability. Shale gas is well known for its extremely low permeability which is only 10^{-3} to 10^{-5} md. This is also the main reason that makes it impossible to recover the gas by conventional methods. According to the data collected, the shale gas matrix permeability in U.S. is mainly distributed between 10^{-3} and 10^{-5} mD. The box plot in Figure 5.6 and histogram in Figure 5.7 give detailed information about matrix permeability data collected.

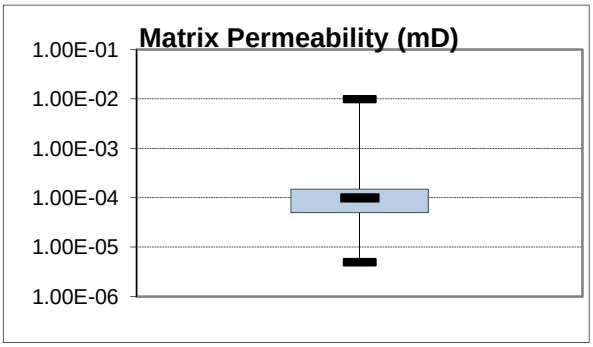

Figure 5.6 Box Plot of Matrix Permeability Data Collected

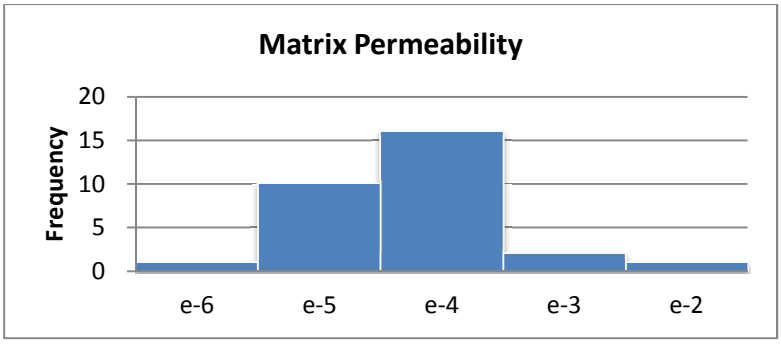

Figure 5.7 Histogram of Matrix Permeability Data Collected

Basing on the data collected, five simulation cases with matrix permeability varying from 10^{-5} mD to 10^{-3} mD have been created and simulated. Figure 5.8 and Figure 5.9 provide simulation result of 20 years cumulative production and gas rate.

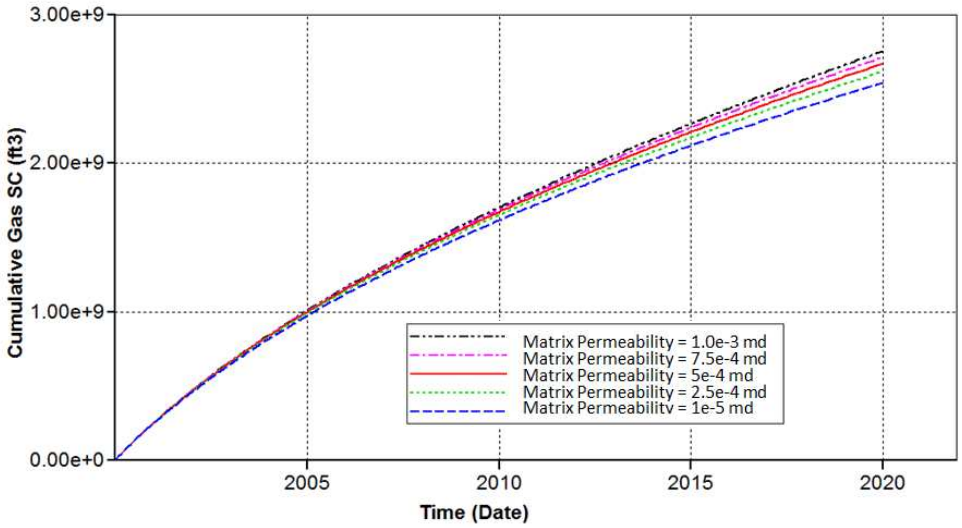

Figure 5.8 Impact of Matrix Permeability to Cumulative Production

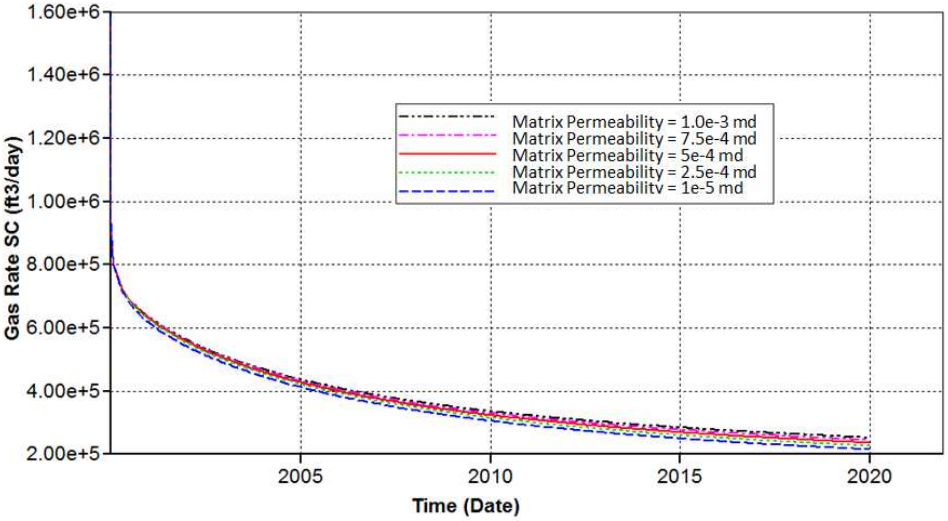

Figure 5.9 Impact of Matrix Permeability to Gas Rate

From the figure above it is clear that the influence of matrix permeability to the gas production rate is very insignificant, the difference between each cases can hardly be distinguished. Even in the cumulative production plot the difference between cases is pretty small. According to the predict of 20 years production, reservoir with 10-3 mD matrix permeability can only produce 213 MMSCF more gas than reservoir with 10-5 mD, which is 7.7% of the whole production.

Since the matrix permeability is one of the most important reasons that block the economic recover of shale gas, it should have significant effect on gas production. However, simulation result shows that the influence of matrix permeability is very limited. The reason of this phenomenon is that although the matrix permeability has been increased to hundreds times, it is still in a relatively low level compared with fracture permeability, which cannot make a big difference to the final result.

5.1.3. Effect of the Natural Fracture Porosity. It is known to all that shale gas reservoir is naturally fractured reservoir. However, according to Julia et al. (2007) natural opening-mode fractures in the Barnett Shale are most commonly narrow, sealed with calcite, and present in an echelon arrays. The narrow fractures are all sealed and cannot contribute to reservoir storage or enhance reservoir conductivity. But, Fisher et al. (2004) and Warpinski et al. (2005) stated that hydraulic fractures stimulation will active and re-open nature fractures; and these re-opened natural fractures will provide pathway for gas flow.

Therefore, it is accepted that natural fracture plays an important role after hydraulic fracture stimulation has been implemented to the reservoir. Different from

matrix, natural fracture has a much higher permeability. Thus, natural fracture should be the main channel for gas flow from matrix to hydraulic fracture and then to wellbore.

In this study, all the existing natural fractures are considered in the open mode. Natural fracture porosity is employed to test the influence of natural fracture to shale gas production. According to published data, the range of natural fracture porosity is assumed to be 0.005 to 0.04.

Figure 5.10 and Figure 5.11 give simulation results of natural fracture porosity sensitivity analysis.

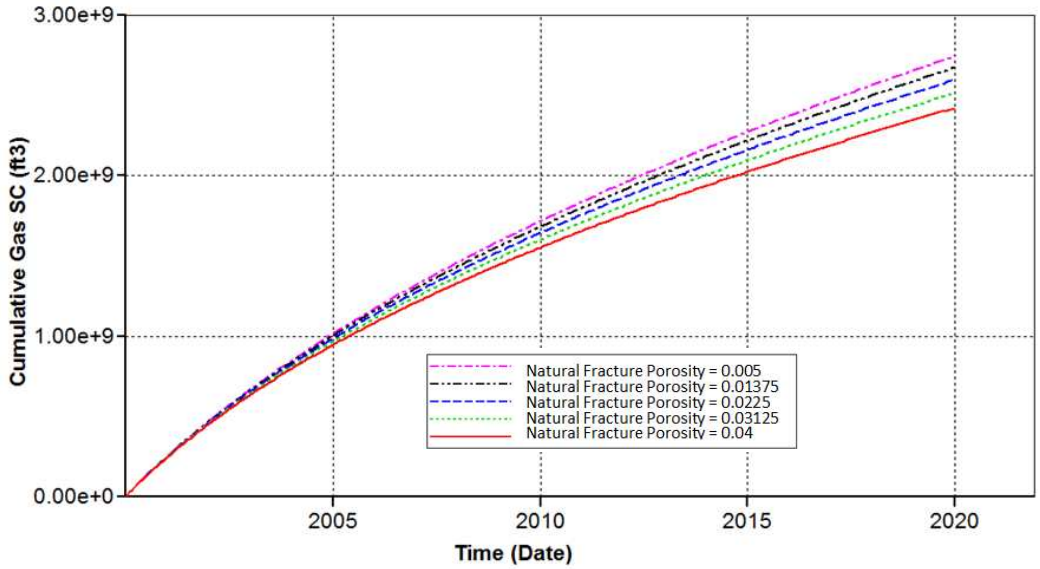

Figure 5.10 Impact of Natural Fracture Porosity to Cumulative Production

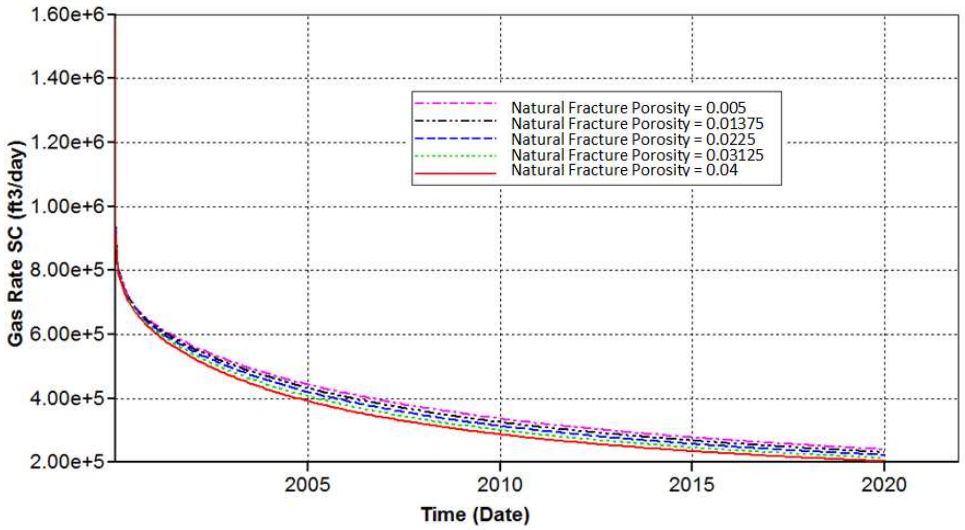

Figure 5.11 Impact of Natural Fracture Porosity to Gas Rate

For 20 years prediction, the case with 3% natural fracture porosity shows 2744 MMSCF cumulative production, and the case with 0.5% natural fracture porosity shows 2421 MMSCF cumulative production, which is 11.8% lower than the 3% one.

5.1.4. Effect of the Rock Compressibility. During gas production, the reservoir pressure will change a lot, and this pressure change will affect properties of reservoir, such as matrix permeability and porosity, fracture permeability and porosity. Thus, it is important to take rock compressibility into consideration. In this study, range of rock compressibility is assumed to be 10^{-6} 1/psi to 10^{-4} 1/psi. Both matrix and fracture have same rock compressibility. Figure 5.12 and Figure 5.13 give simulation results of rock compressibility sensitivity analysis.

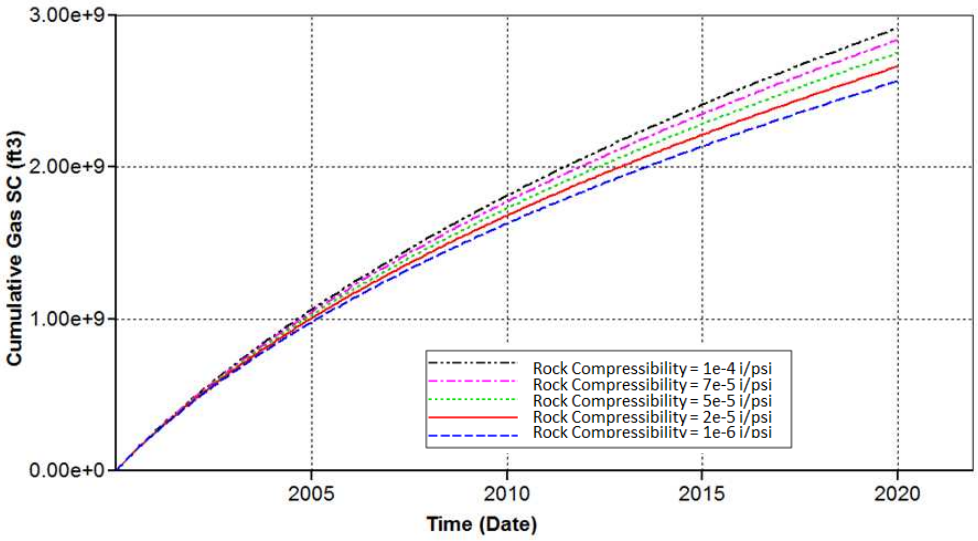

Figure 5.12 Impact of Rock Compressibility to Cumulative Gas Production

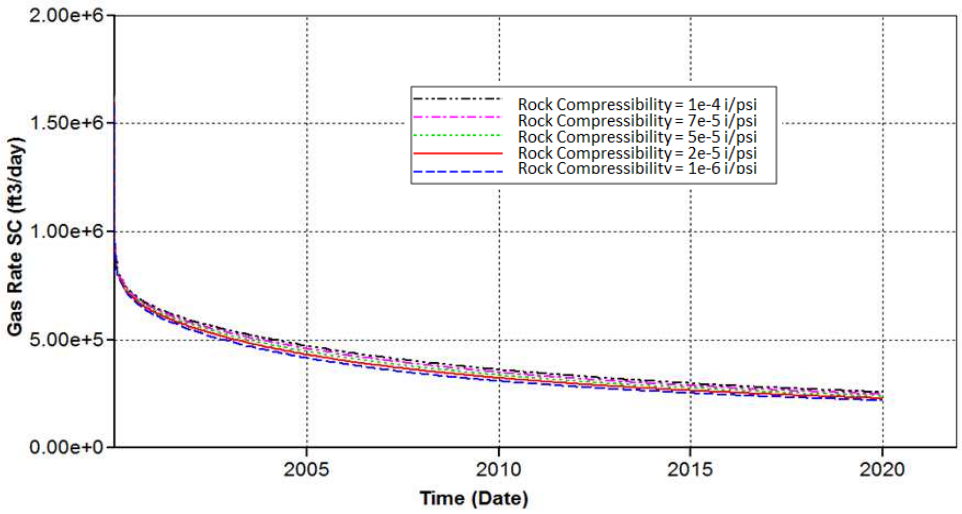

Figure 5.13 Impact of Rock Compressibility to Gas Rate

Basing on the simulation result, the 20 years cumulative production of reservoir with 1e-4 1/psi is 2915 MMSCF, and the 20 years cumulative production of reservoir with 1e-6 rock compressibility is 2566 MMSCF. A 12.0% difference has been achieved between the lowest rock compressibility and the highest one.

5.1.5. Effect of the Gas Desorption. According to the Langmuir isotherm equation, except reservoir pressure, gas desorption process is controlled by two parameters: Langmuir Volume and Langmuir Pressure. In this section, the influence of Langmuir volume and Langmuir pressure were analyzed individually first then as combined.

5.1.5.1 Effect of the Langmuir pressure. Langmuir pressure is the pressure when the amount of gas adsorbed is half of the Langmuir volume. The box plot in Figure 5.14 and histogram in Figure 5.15 show the distribution of Langmuir pressure data.

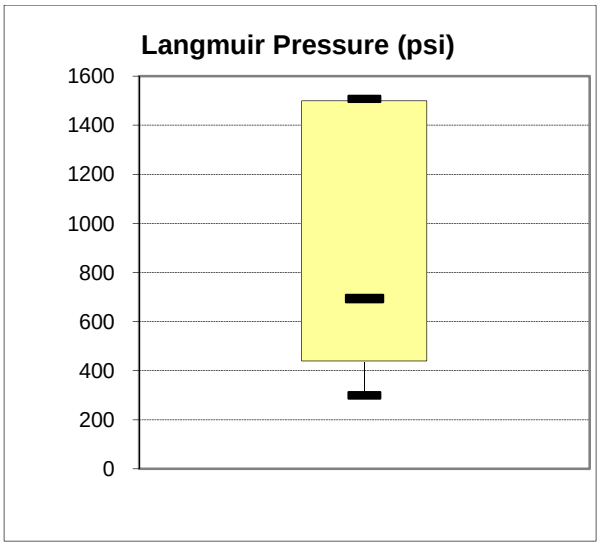

Figure 5.14 Box Plot of Langmuir Pressure Data Collected

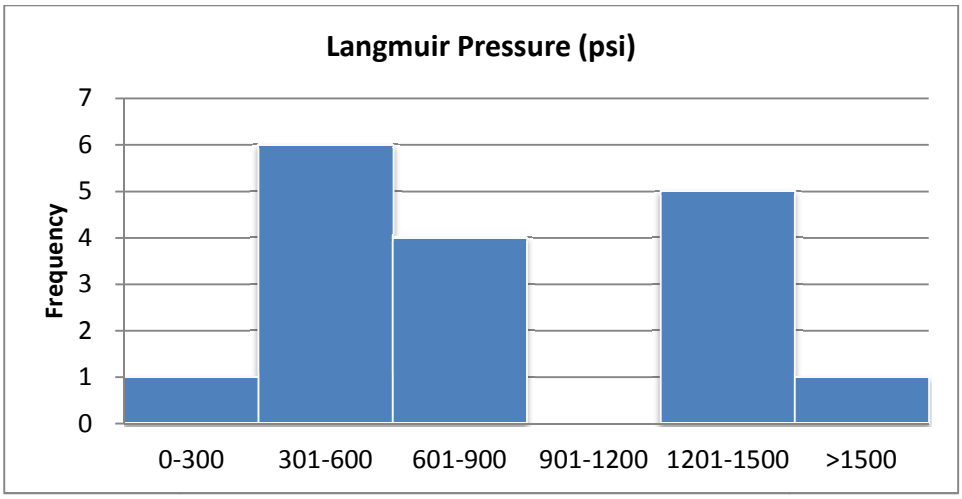

Figure 5.15 Histogram of Langmuir Pressure Data Collected

Basing on the two figures above, a range of 400 psi to 1500 psi for Langmuir Pressure has been determined. For this part, Langmuir volume has been fixed at 100 SCF/ton. Figures 5.16 and 5.17 present the sensitivity analysis results of Langmuir pressure.

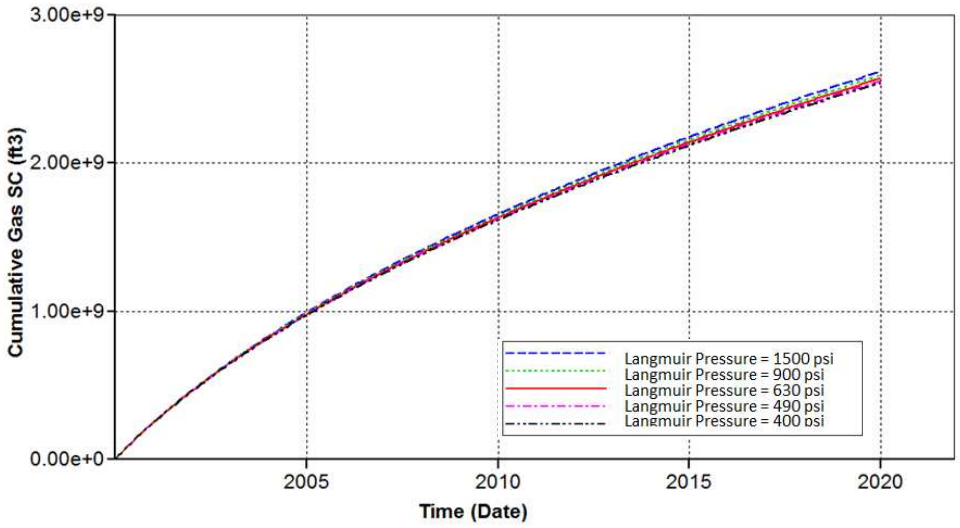

Figure 5.16 Impact of Langmuir Pressure to Cumulative Gas Production

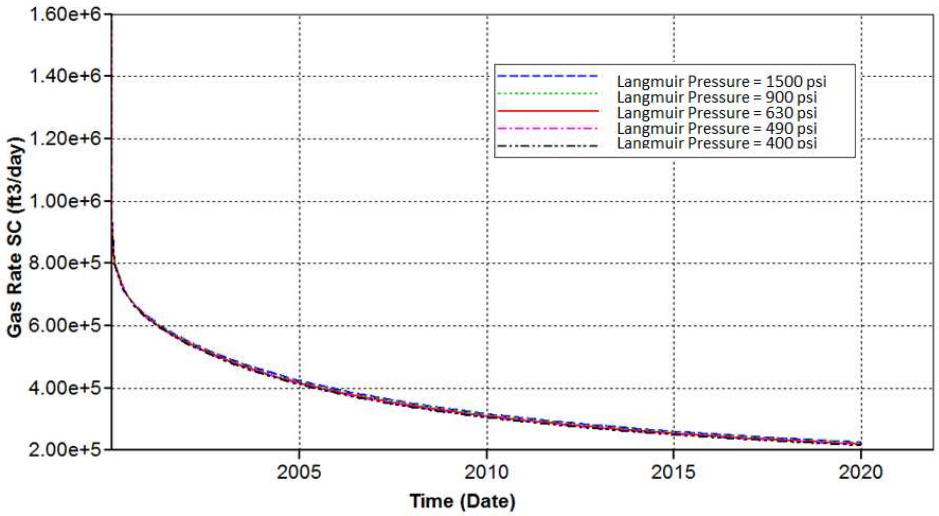

Figure 5.17 Impact of Langmuir Pressure to Gas Rate

5.1.5.2 Effect of the Langmuir volume. Langmuir volume is the maximum amount of gas that can be adsorbed on the rock surface under infinite pressure. The box plot in Figure 5.18 and histogram in Figure 5.19 show the distribution of Langmuir volume data.

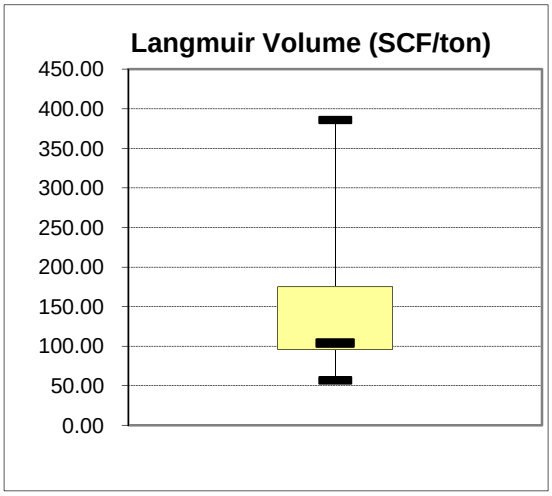

Figure 5.18 Box Plot of Langmuir Volume Data Collected

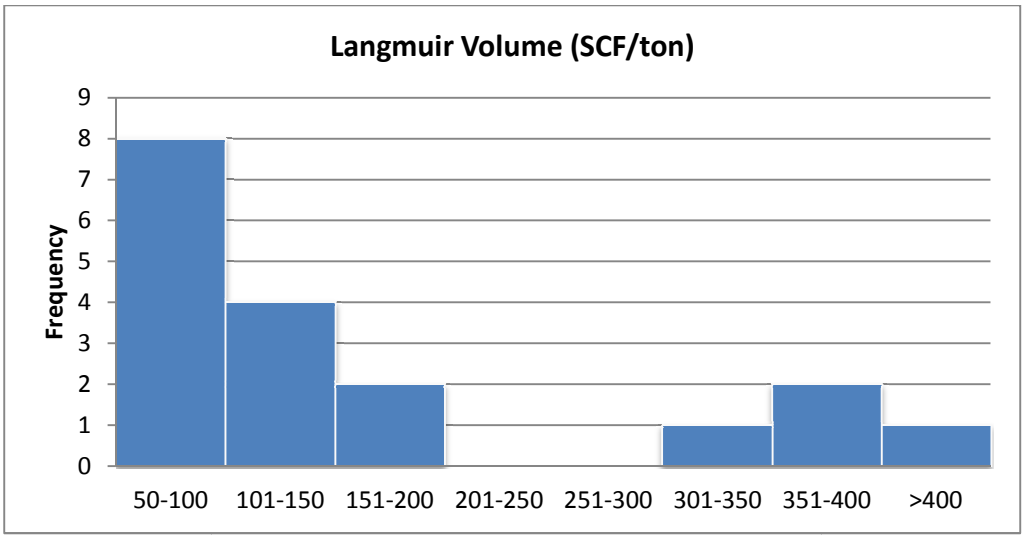

Figure 5.19 Histogram of Langmuir Volume Data Collected

Basing on two figures above, a range of 60 SCF/ton to 220 SCF/ton has been determined for sensitivity analysis. For this part, Langmuir pressure has been fixed at 650 psi. Figures 5.20 and 5.21 present the sensitivity analysis results of Langmuir pressure.

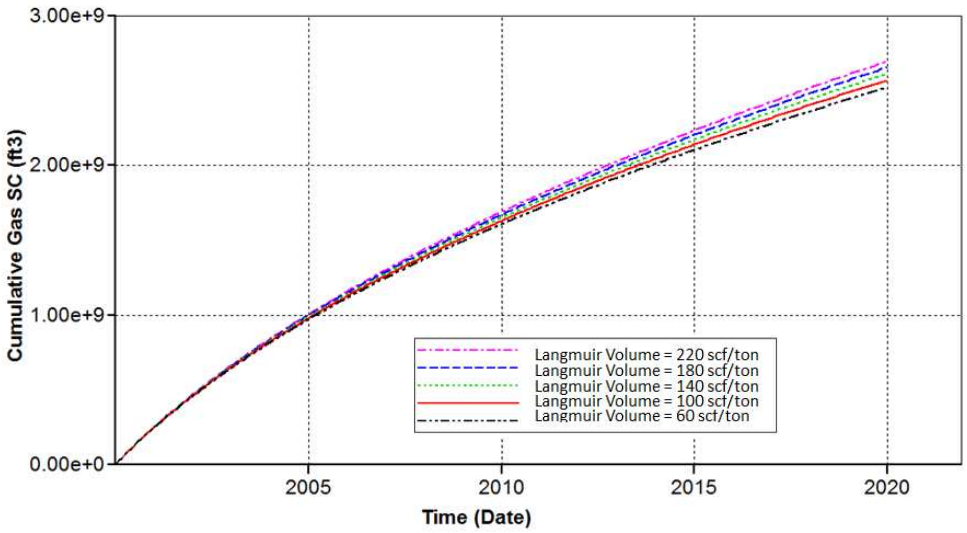

Figure 5.20 Impact of Langmuir Volume to Cumulative Gas Production

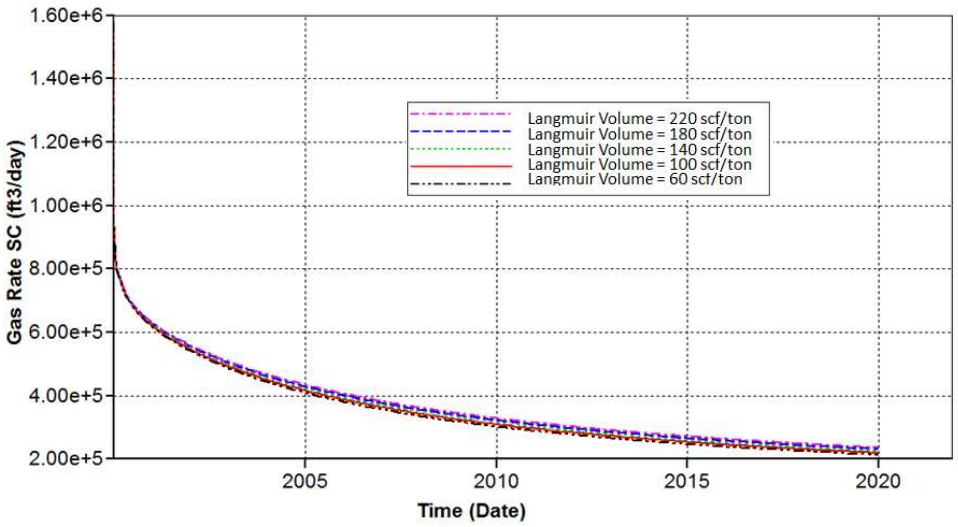

Figure 5.21 Impact of Langmuir Volume to Gas Rate

5.1.5.3 Overall effect of the gas desorption. For study the influence of gas desorption to shale gas recover, three cases have been designed basing on different Langmuir volume and Langmuir pressure, as shown in Table 5.2.

Table 5.2 Langmuir Volume and Langmuir Pressure Values for Gas Desorption Sensitivity Analysis

	Case 1	Case 2	Case 3	No Gas Desorption
Langmuir Pressure (psi)	400	1000	1500	N/A
Langmuir Volume (scf/ton)	60	140	220	N/A
20 yr. Cumulative Production(MMSCF)	2504	2646	2775	2449

From Figure 5.22, it can be seen that gas desorption will increase 2.2% - 13.3% of the 20 yr. ultimate gas production which means that for reservoir with different Langmuir parameters the results will be dramatically different. At the same time, desorbed gas is mainly produced during late time of production. So whether or not the gas desorption should be taken into consider is depends on economic limits and reservoir properties.

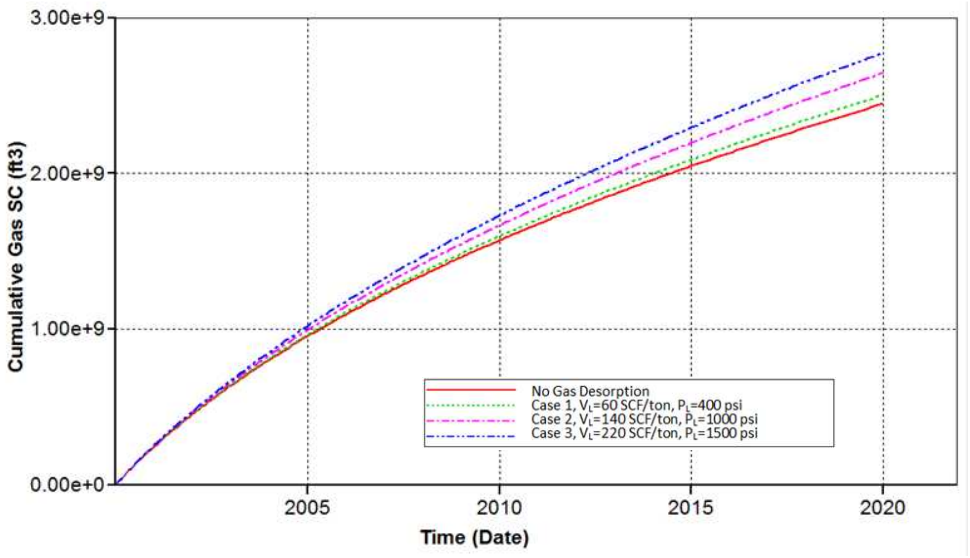

Figure 5.22 Impact of Gas Desorption to Cumulative Gas Production

5.1.6. Sensitivity Analysis for All Reservoir Parameters. In this part, all six reservoir parameters mentioned above are considered together.

Ranges of parameters are provided in the Table 5.3. DOE (Design of Experiments method) is applied to generate 224 experiments for creating the proxy model.

Table 5.3 Reservoir Parameters and their Value Range for Sensitivity Analysis

Parameter	Value	Unit
Langmuir Pressure	400 - 1500	psi
Langmuir Volume	60 - 220	SCF/ton
Matrix Porosity	0.025 – 0.10	
Matrix Permeability	1e-3 – 1e-5	md
Rock compaction	1e-4 – 1e-6	psi-1
Natural Fracture Porosity	0.005 – 0.04	

Reduced Quadratic proxy model for reservoir parameters:

$$C_{G_P} = 1.15522 * 10^9 + 3.06922 * 10^{12} * CPOR - 7.43388 * 10^{10} * LangP + 4.50303 * 10^9 * LangV + 3.36108 * 10^{11} * MPERM + 2.02781 * 10^{10} * MPOR + 2.22082 * 10^{10} * NFPOR - 2.85072 * 10^{15} * CPOR * CPOR - 6.30267 * 10^{12} * CPOR * LangV + 1.11318 * 10^{13} * CPOR * MPOR + 1.43965 * 10^{13} * CPOR * NFPOR + 1.1181 * 10^{13} * LangP * LangP - 5.04848 * 10^{11} * LangP * LangV + 4.14465 * 10^{11} * LangP * MPOR + 3.43468 * 10^{11} * LangP * NFPOR - 1.97262 * 10^{10} * LangV * MPOR - 2.61703 * 10^{10} * LangV * NFPOR - 9.55955 * 10^{13} * MPERM * MPERM - 4.39757 * 10^{11} * MPERM * MPOR - 5.97771 * 10^{11} * MPERM * NFPOR - 5.08726 * 10^{10} * MPOR * MPOR - 1.24145 * 10^{11} * MPOR * NFPOR - 8.29543 * 10^{10} * NFPOR * NFPOR \quad (6)$$

MPOR – matrix porosity, CPOR – rock compressibility, NFPOR – natural fracture porosity, MPERM – matrix permeability, LangV – Langmuir volume, LangP – Langmuir pressure.

Figure 5.23 shows the result of proxy analysis of cumulative production. Value after each parameter is the expected increase of cumulative production by changing that parameter from lowest to highest. So, the larger the value is, the more important the parameter will be.

From the result, it is clear that matrix porosity is the most important parameter for 20 years cumulative production, after that is rock compressibility, natural fracture porosity, matrix permeability, Langmuir volume, and Langmuir pressure. Maximum is the maximum cumulative production by using provided ranges of parameters. Minimum is the minimum cumulative production by using provided ranges of parameters. In this figure, the unit of Langmuir volume is gmole/lb, and the unit of Langmuir pressure is 1/psi.

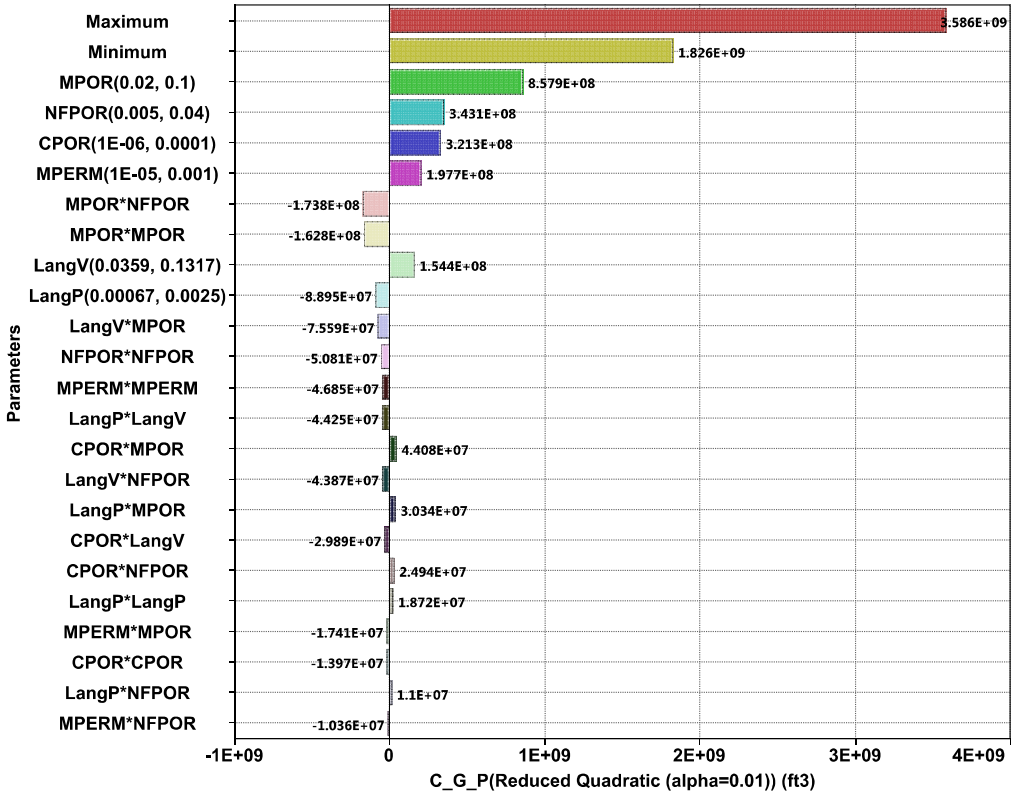

Figure 5.23 Tornado Plot of Effect Estimate for Reservoir Parameters

MPOR – matrix porosity, CPOR – rock compressibility, NFPOR – natural fracture porosity, MPERM – matrix permeability, LangV – Langmuir volume, LangP – Langmuir pressure.

In Figure 5.24, result from simulation has been organized and presented with percentage of contribution to cumulative production changing. Langmuir volume and Langmuir pressure are combined together and treated as one parameter, because both of them are used to describe the influence of gas desorption.

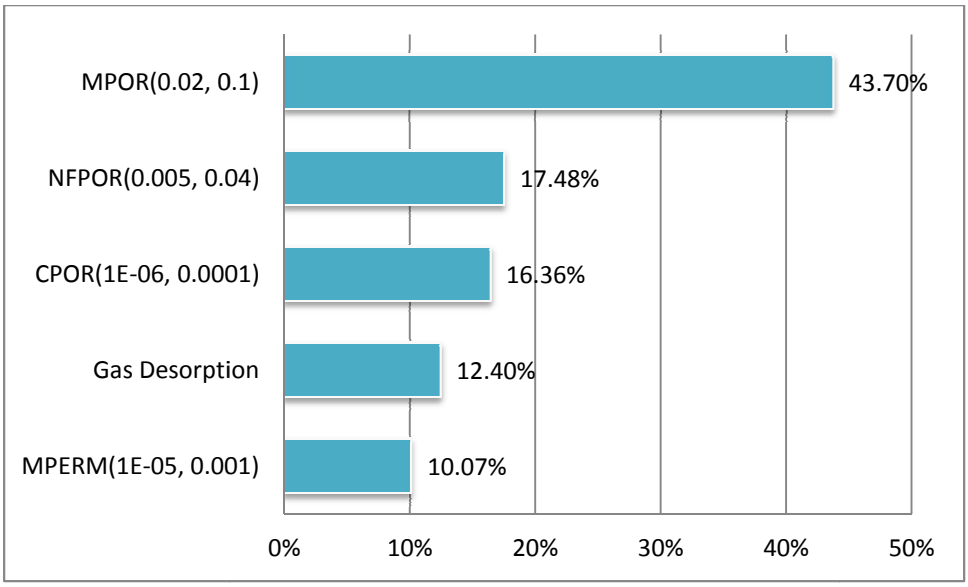

Figure 5.24 Weights of Each Reservoir Parameters to Cumulative Production

Among all reservoir parameters tested in study, matrix porosity is the most important parameter which is 43.70% weight, natural fracture and rock compressibility have similar weights which are 17.48% and 16.36%, gas desorption and matrix permeability have relatively small weight, 12.40% and 10.07%.

5.2. SENSITIVITY ANALYSIS OF HYDRAULIC FRACTURE PARAMETERS

In this section, influence of each hydraulic fracture parameter will be studied separately. After that, all the parameters will be put together to analyze interplay between them. Parameters studied in this section include: hydraulic fracture half-length, hydraulic fracture height, hydraulic fracture conductivity, and hydraulic fracture spacing. Figure 5.25 gives explanation of hydraulic fracture parameters.

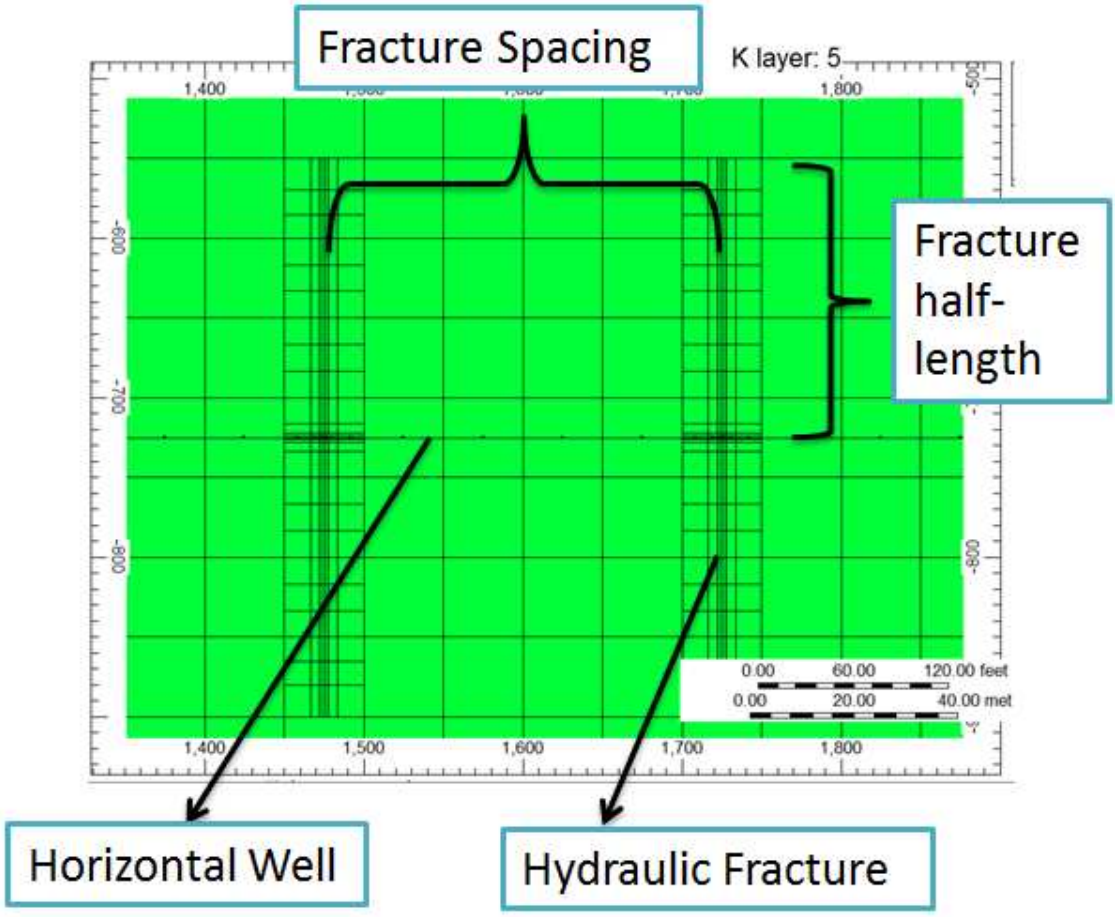

Figure 5.25 Explanation of Hydraulic Fracture Parameters

5.2.1. Effect of the Hydraulic Fracture Half-length. Hydraulic fracture half-length is the horizontal distance from horizontal wellbore to the end of hydraulic fracture. In this research, relationship of shale gas production and hydraulic fracture half-length is performed by changing hydraulic fracture half-length from 100ft to 500ft. Figures 5.26 and 5.27 show the influence of hydraulic fracture half-length to cumulative production and gas rate.

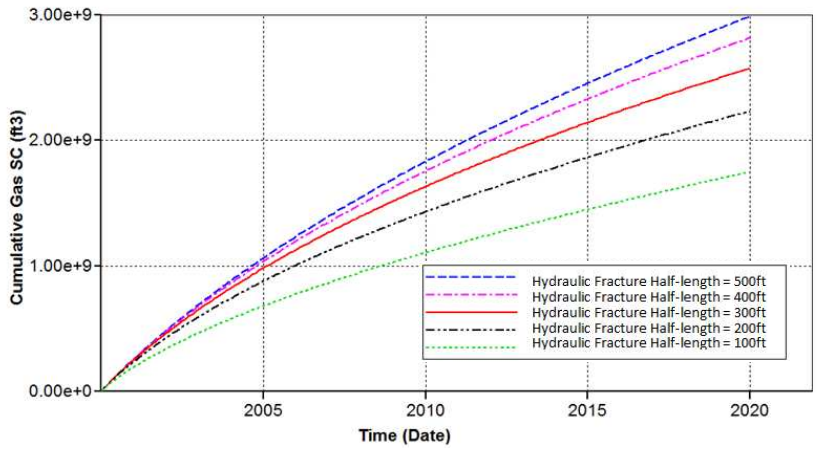

Figure 5.26 Impact of Hydraulic Fracture Half-Length to Cumulative Production

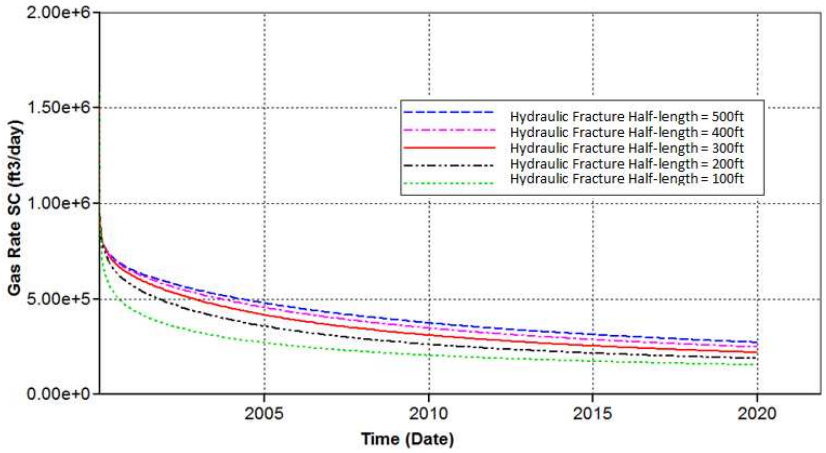

Figure 5.27 Impact of Hydraulic Fracture Half-Length to Gas Rate

From Figures 5.26 and 5.27, it is clear that although the cumulative production and gas rate will increase with the increase of fracture half-length, the increase of cumulative production is not proportional to the increase of fracture half-length. Increasing fracture half-length from 100ft to 200ft can enhance 484 MMSCF to cumulative production; however, increasing fracture half-length from 200ft to 300ft can only enhance 341 MMSCF to cumulative production. That means increasing the fracture

half-length do will enhance cumulative production, but the improvement of production will gradually decrease with the increases of fracture half-length.

Figure 5.28 compares pressure distribution of fracture half-length equal to 100ft and 500ft for twenty year production. It is clear that in both two cases, the pressure transition does not reach the reservoir boundary so that the phenomenon mentioned above is not on account of limitation of reservoir size.

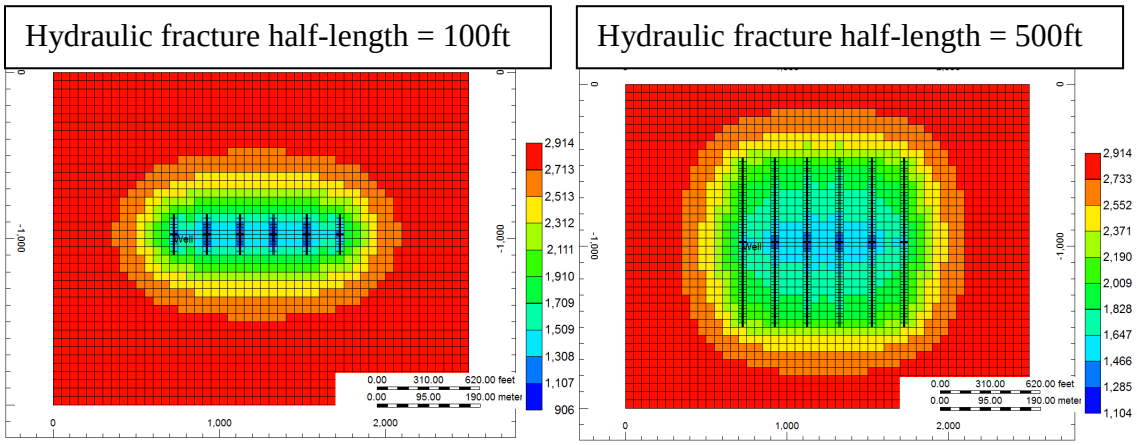

Figure 5.28 Pressure Distribution of Hydraulic Fracture Half-Length L_f=100ft and L_f=500ft for Twenty Year Production

5.2.2. Effect of the Hydraulic Fracture Height. Since the reservoir thickness is 300ft, the upper limit of hydraulic fracture height is set as 300ft. The candidates value of sensitivity analysis for hydraulic fracture height are 100ft, 150ft, 200ft, 250ft, and 300ft. Figures 5.29 and 5.30 show the result of sensitivity analysis of hydraulic fracture height.

From the figure below, it is clear that hydraulic fracture height shows similar trend with hydraulic fracture half-length. With increasing of fracture height, the cumulative production will also increase, but the increasing rate will decrease when

fracture height comes to high level. Different with fracture half-length, limitation of reservoir dimension is one of the most important reasons for this phenomenon.

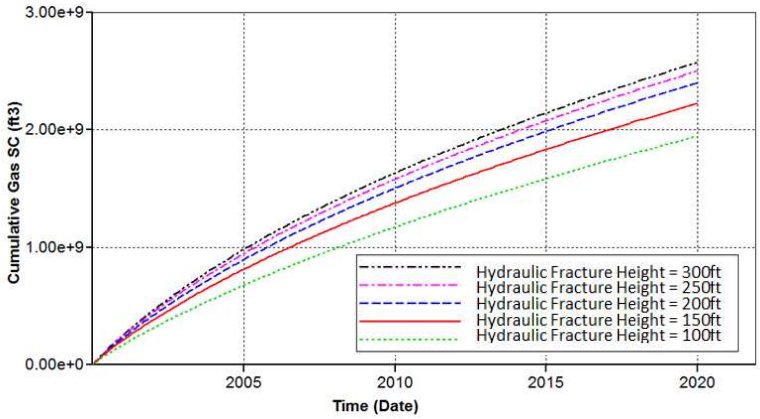

Figure 5.29 Impact of Hydraulic Fracture Height to Cumulative Production

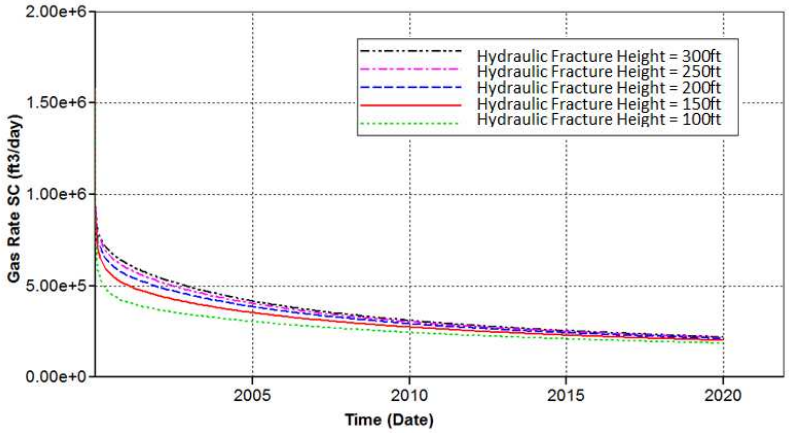

Figure 5.30 Impact of Hydraulic Fracture Height to Gas Rate

5.2.3. Effect of the Hydraulic Facture Spacing. When placing multiple transverse fractures in shale gas reservoirs, it is crucial to minimize the spacing between fractures in order to achieve commercial production rates and an optimum depletion of the reservoir (Cipolla et al. 2009). The fracture spacing determines the number of fractures along the horizontal wellbore; and the more hydraulic fractures, the bigger the

stimulated reservoir volume, the greater the production. However, due to economic and geomechanics limitation, it is infeasible to infinitely increase the number of hydraulic fractures.

Figures 5.31 and 5.32 depict the impact of hydraulic fractures to the cumulative production. Fracture spacing of 100ft, 200ft, 300ft, and 500ft have been selected for the sensitivity analysis. Since the length of horizontal well is 1000ft, case with 400ft and 500ft will have same number of fractures, and case with 400ft spacing was abandoned.

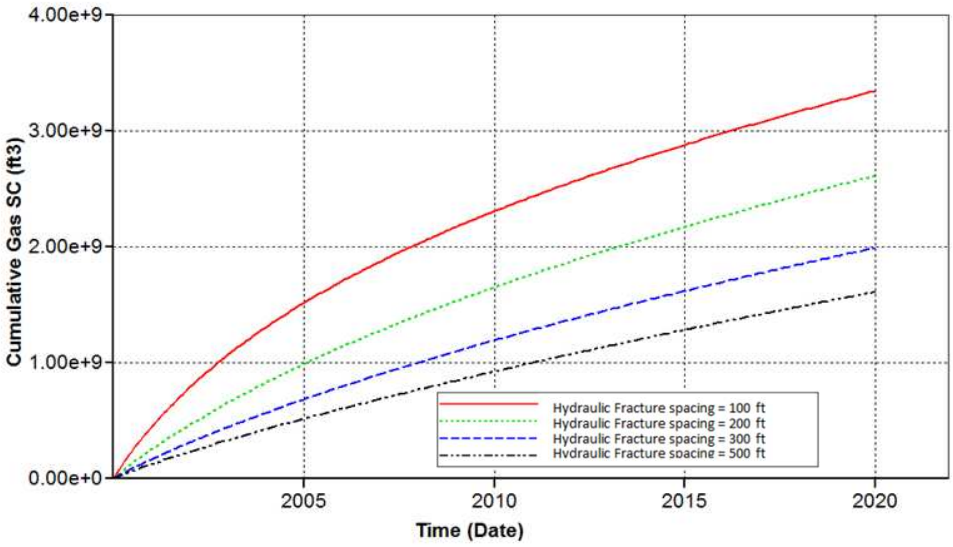

Figure 5.31 Impact of Hydraulic Fracture Spacing to Cumulative Production

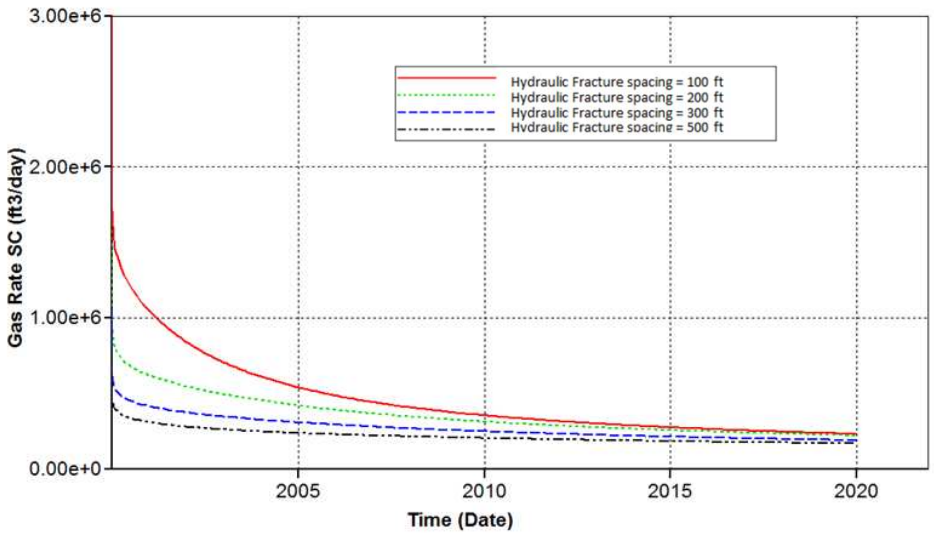

Figure 5.32 Impact of Hydraulic Fracture Spacing to Gas Rate

From Figure 5.31 and Figure 5.32, it is clear that hydraulic fracture spacing has enormous influence to shale gas production. By changing fracture spacing from 200ft to 100ft, cumulative production will increase from 2612 MMSCF to 3344 MMSCF which is increased 28.0%; and for the gas rate, although at the end of 2020 (20 years) the difference on gas rate between cases is relatively small, but within the first ten years there are significant differences between them.

Figure 5.33 shows the pressure distributions for 100ft case and 200ft case. It is clear that case with 100ft fracture spacing has larger pressure drops than the case with 200ft. At the same time, it can be seen from this figure that the difference of areas of pressure drop between 100ft case and 200ft is not very big.

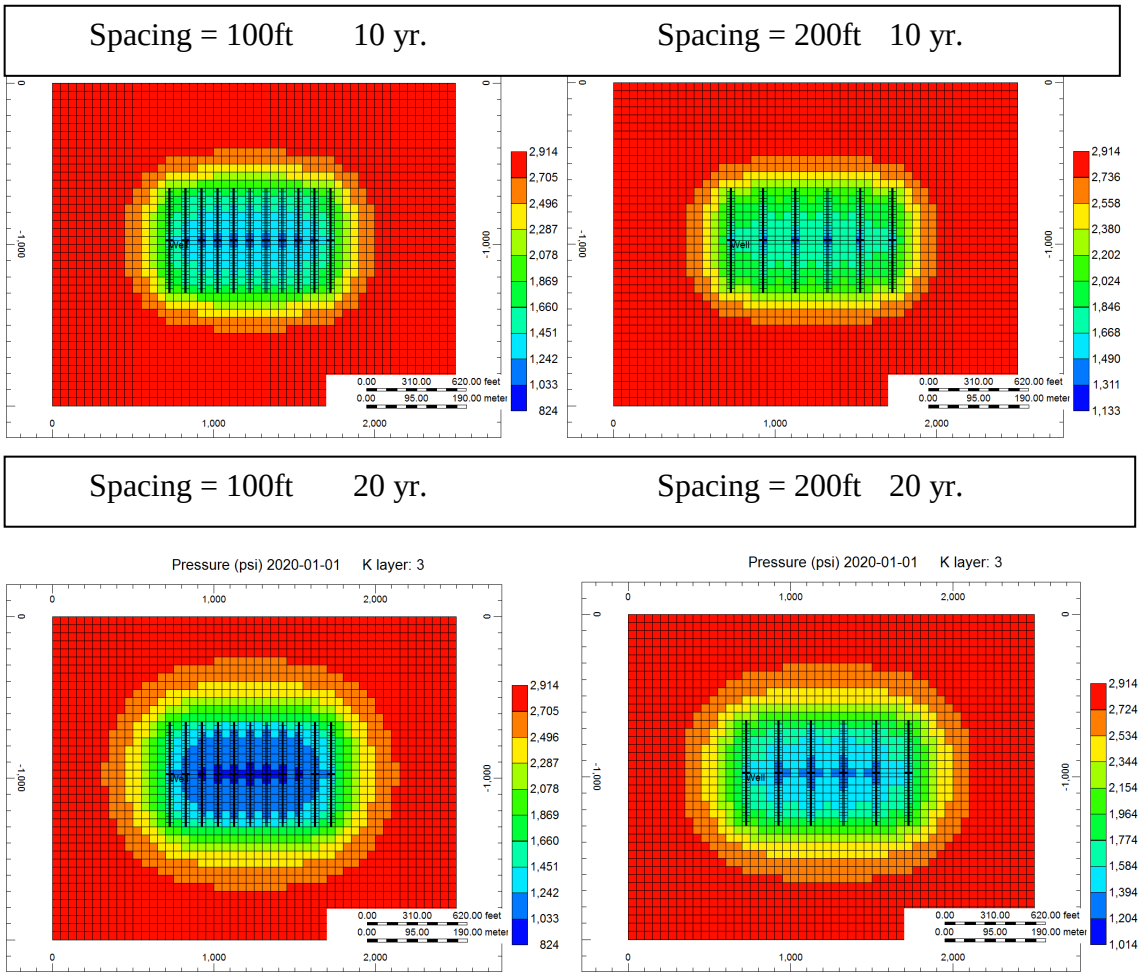

Figure 5.33 Pressure Distributions after 10 Years and 20 Years for Fracture Spacing L_s=100ft and L_s=200ft

5.2.4. Effect of the Hydraulic Fracture Conductivity. Hydraulic fracture conductivity is defined as the product of hydraulic fracture width and permeability. It is an important parameter to evaluate the quality of hydraulic fracture.

In this model, changing of fracture conductivity is accomplished by varying permeability of hydraulic fracture. Five options of 1 md*ft, 3 md*ft, 5 md*ft, 7 md*ft, and 9 md*ft are selected for sensitivity analysis.

Figure 5.34 shows the impact of hydraulic fracture conductivity to cumulative production. It is obvious that the fracture conductivity has significant influence on the

cumulative production. When the fracture conductivity is enhanced from 1 md*ft to 3 md*ft, the cumulative production is dramatically increased from 1834 MMSCF to 2996 MMSCF, which increased 63%. After that, from 3 md*ft to 9 md*ft, growth rate is gradually decreased.

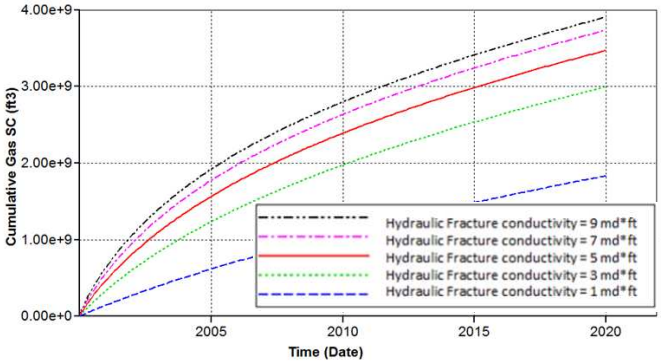

Figure 5.34 Impact of Hydraulic Fracture Conductivity to Cumulative Production

Figure 5.35 shows that, except the case with 1 md*ft, the differences of gas production between cases is mainly existing in the first 10 years of production. After 20 years, there is almost no difference between cases with fracture conductivity ranging from 3 md*ft to 9 md*ft.

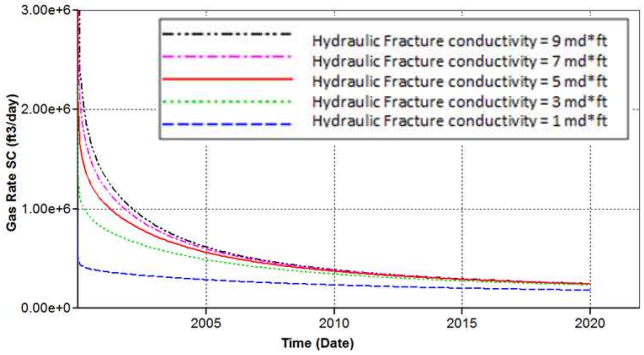

Figure 5.35 Impact of Hydraulic Fracture Conductivity to Gas Rate

5.2.5. Hydraulic Fracture Parameters Sensitivity Analysis. In this section, sensitivity analysis was applied to all above mentioned hydraulic fracture parameters to determine their impact to shale gas production. CMOST was applied for hydraulic fracture parameters sensitivity analysis. A reduced quadratic model was created by using response surface methodology to estimate the effect of each parameter. 117 job patterns were generated for creating the proxy model. Table 5.4 gives a summary of range of hydraulic fracture parameters.

Table 5.4 Hydraulic Fracture Parameters and Their Range Values for Sensitivity Analysis

Parameter	Value	Unit
Hydraulic Fracture Half-length	100 - 500	ft
Hydraulic Fracture Height	100 - 300	ft
Hydraulic Fracture Spacing	100 - 500	ft
Hydraulic Fracture Conductivity	1 - 9	mD*ft

Below is the reduced quadratic model equation in terms of actual parameters:

$$\begin{aligned} Cumulative\ Gas\ Production &= 5.12972 * 10^8 - 6.55292 * 10^6 * SPACING + 5.74939 * 10^6 \\ &* HALFLENGTH + 7.43302 * 10^6 * HEIGHT + 2.42412 * 10^8 \\ &* CONDUCTIVITY + 10532.8 * SPACING * SPACING - 7992.47 \\ &* SPACING * HALFLENGTH - 5294.03 * SPACING * HEIGHT \\ &- 136947 * SPACING * CONDUCTIVITY - 5376.94 * HALFLENGTH \\ &* HALFLENGTH + 5768.71 * HALFLENGTH * HEIGHT + 581001 \\ &* HALFLENGTH * CONDUCTIVITY - 12921.3 * HEIGHT * HEIGHT \\ &+ 281159 * HEIGHT * CONDUCTIVITY - 2.48022 * 10^7 \\ &* CONDUCTIVITY * CONDUCTIVITY \end{aligned} \quad (7)$$

SPACING – Hydraulic fracture spacing;

HALFLENGTH – Hydraulic fracture half-length;

HEIGHT – Hydraulic fracture height;

CONDUCTIVITY – Hydraulic fracture conductivity.

Figure 5.36 and Figure 5.37 give the result of response surface methodology.

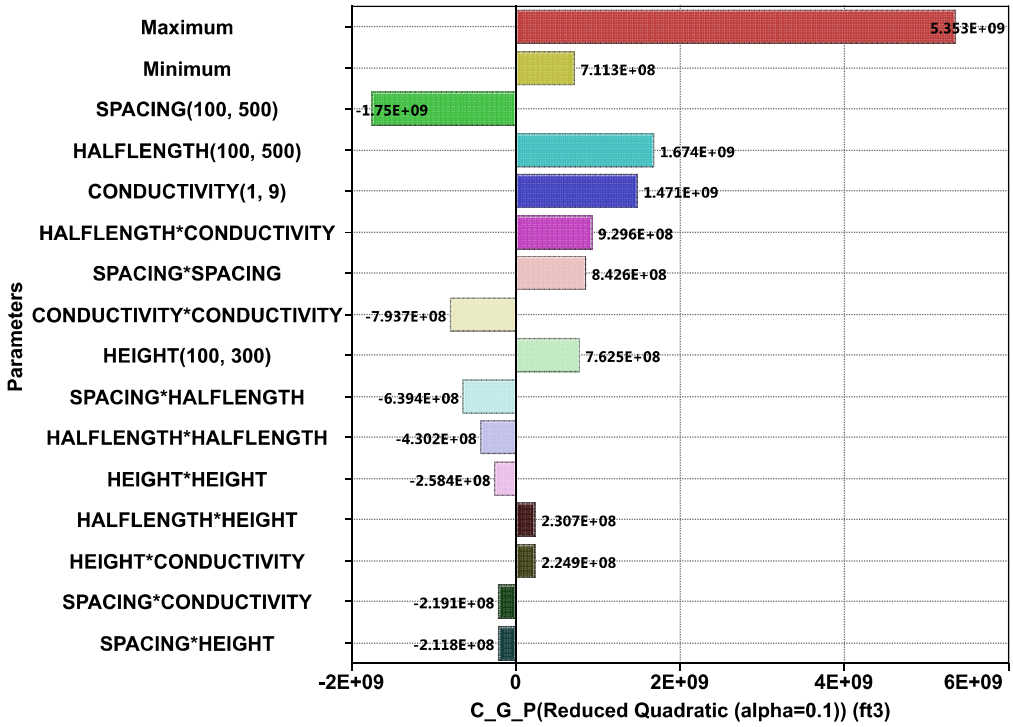

Figure 5.36 Tornado Plot of Effect Estimate for Hydraulic Fracture Parameters

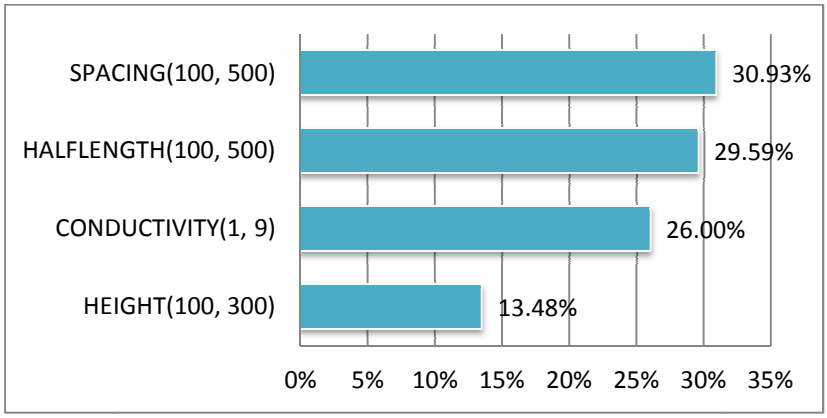

Figure 5.37 Weights of Hydraulic Fracture Parameters to Cumulative Production

From the simulation result above, it is clear that for 20 years production hydraulic fracture spacing is the most important parameter, which has a weight of 30.93%. Hydraulic fracture half-length and conductivity have similar effect to the cumulative production. Fracture height, due to the limitation of reservoir thickness, has the lowest influence to production.

5.3. SENSITIVITY ANALYSIS FOR ALL PARAMETERS

After analyzing the impact of individual reservoir and hydraulic fracturing parameters on shale gas production separately and grouping, effects of parameters for 1, 5, 10, and 20 years cumulative production will be ranked. Latin hypercube design is used for creating simulation jobs. For each sensitivity study, 534 jobs have been generated to build up proxy model for effect estimate for each case.

5.3.1. One Year Production Test. Simulation results (Figure 5.38 and Figure 5.39) show that in the first year, cumulative production is dominated by hydraulic fracture parameters, four kinds of hydraulic fracture properties occupy top 4 in effect ranking. Hydraulic fracture spacing is no doubt the most important factor in the first year's production, which is 33.67 %. After that is hydraulic fracture conductivity with 26.63 %. Hydraulic fracture half-length and height have similar effect, which is 12.76 % and 11.68 %. All effects of reservoir parameters are below 5 %.

$$
\begin{aligned}
&Cumulative\ Production \\
&\quad = -5.38522 * 10^7 + 4.78312 * 10^7 * CONDUCTIVITY + 909298 \\
&\quad * HALFLENGTH + 1.72444 * 10^6 * HEIGHT - 1.72132 * 10^6 \\
&\quad * SPACING + 1.04915 * 10^{11} * CPOR - 6.70741E + 09 * LANGP \\
&\quad - 4.62259E + 08 * LANGV + 1.72443 * 10^{11} * MPERM + 1.21263 \\
&\quad * 10^9 * MPOR + 1.83744 * 10^9 * NFPOR - 4.06013 * 10^6 \\
&\quad * CONDUCTIVITY * CONDUCTIVITY + 86207.6 * CONDUCTIVITY \\
&\quad * HALFLENGTH + 117342 * CONDUCTIVITY * HEIGHT - 116925 \\
&\quad * CONDUCTIVITY * SPACING + 5.58077 * 10^{10} * CONDUCTIVITY \\
&\quad * CPOR + 4.82399 * 10^7 * CONDUCTIVITY * LANGV + 4.39438E \\
&\quad * 10^9 * CONDUCTIVITY * MPERM + 1.50742 * 10^8 \\
&\quad * CONDUCTIVITY * MPOR + 1.06968 * 10^8 * CONDUCTIVITY \\
&\quad * NFPOR - 1117.38 * HALFLENGTH * HALFLENGTH + 531.592 \\
&\quad * HALFLENGTH * HEIGHT - 1244.96 * HALFLENGTH * SPACING \\
&\quad - 2986.28 * HEIGHT * HEIGHT - 2069.39 * HEIGHT * SPACING \\
&\quad + 1.80522 * 10^6 * HEIGHT * LANGV - 1.37453 * 10^8 * HEIGHT \\
&\quad * MPERM + 3941.09 * SPACING * SPACING - 5.77318 * 10^8 \\
&\quad * SPACING * CPOR - 1.34826 * 10^8 * SPACING * MPERM - 2.98441 \\
&\quad * 10^6 * SPACING * MPOR - 2.56049E + 06 * SPACING * NFPOR \\
&\quad - 6.22371 * 10^{13} * MPERM * MPERM - 1.50691 * 10^{10} * MPOR \\
&\quad * NFPOR
\end{aligned} \tag{8}
$$

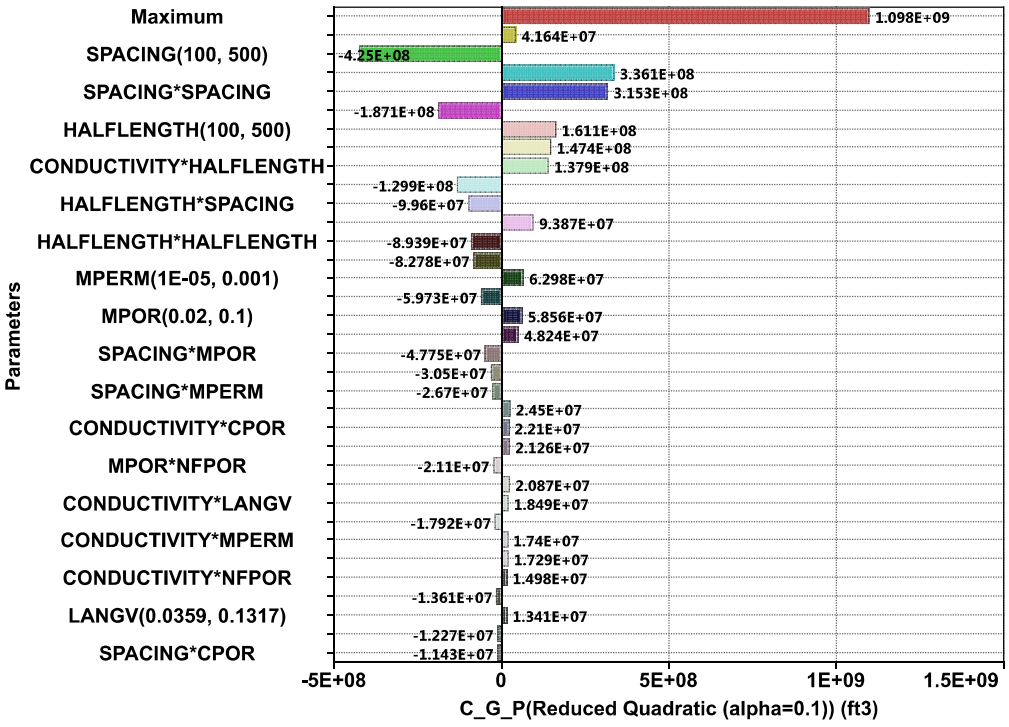

Figure 5.38 Tornado Plot of Effect Estimate for First Year Cumulative Production

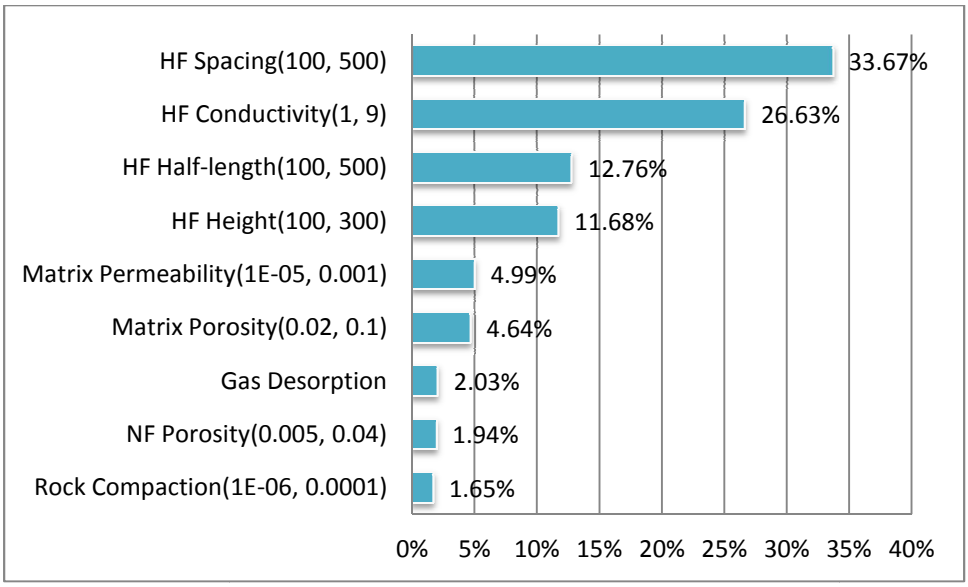

Figure 5.39 Weights of Parameters to First Year Cumulative Production

5.3.2. Five Years Production Test. As shown in Figure 5.40 and Figure 5.41, similar to effect estimate results for first year, according to effect estimate for five years, hydraulic fracture properties are still dominate factors for cumulative production. However compared with the result of first year analysis, the effects of hydraulic fracture spacing and conductivity have slight decrease; on the other hand, hydraulic fracture height and half-length increase a little. Effects of reservoir parameters are still in a pretty low level. Overall, for short term production, hydraulic fracture is the most important factor that can influence the cumulative production.

$$C_{G_P} = -2.38182 * 10^8 + 1.18359 * 10^8 * \text{CONDUCTIVITY} + 1.41984 * 10^{12} * \text{CPOR} + 2.51456 * 10^6 * \text{HALFLENGTH} + 2.56038 * 10^6 * \text{HEIGHT} - 3.73704E + 10 * \text{LANGP} + 1.38984 * 10^9 * \text{LANGV} + 3.80536 * 10^{11} * \text{MPERM} + 7.66449 * 10^9 * \text{MPOR} + 2.11814 * 10^9 * \text{NFPOR} - 3.42637 * 10^6 * \text{SPACING} - 1.31305 * 10^7 * \text{CONDUCTIVITY} * \text{CONDUCTIVITY} + 299878 * \text{CONDUCTIVITY} * \text{HALFLENGTH} + 307221 * \text{CONDUCTIVITY} * \text{HEIGHT} + 3.15731 * 10^{10} * \text{CONDUCTIVITY} * \text{MPERM} + 5.78621 * 10^8 * \text{CONDUCTIVITY} * \text{MPOR} + 4.85427 * 10^8 * \text{CONDUCTIVITY} * \text{NFPOR} - 258555 * \text{CONDUCTIVITY} * \text{SPACING} + 4.72441 * 10^9 * \text{CPOR} * \text{HEIGHT} - 4.20506 * 10^9 * \text{CPOR} * \text{SPACING} - 2912.94 * \text{HALFLENGTH} * \text{HALFLENGTH} + 3317.65 * \text{HALFLENGTH} * \text{HEIGHT} - 2.37481 * 10^8 * \text{HALFLENGTH} * \text{MPERM} + 6.46701 * 10^6 * \text{HALFLENGTH} * \text{MPOR} + 5.99729 * 10^6 * \text{HALFLENGTH} * \text{NFPOR} - 5266.09 * \text{HALFLENGTH} * \text{SPACING} - 6511.93 * \text{HEIGHT} * \text{HEIGHT} + 9.76165 * 10^6 * \text{HEIGHT} * \text{MPOR} + 1.22961 * 10^7 * \text{HEIGHT} * \text{NFPOR} - 4717.91 * \text{HEIGHT} * \text{SPACING} - 5.8313 * 10^{11} * \text{LANGP} * \text{MPOR} + 1.31569 * 10^8 * \text{LANGP} * \text{SPACING} - 1.52376 * 10^{10} * \text{LANGV} * \text{MPOR} - 9.37857 * 10^{13} * \text{MPERM} * \text{MPERM} - 3.76508 * 10^8 * \text{MPERM} * \text{SPACING} - 2.46438 * 10^{10} * \text{MPOR} * \text{MPOR} - 1.92813 * 10^7 * \text{MPOR} * \text{SPACING} - 1.598 * 10^7 * \text{NFPOR} * \text{SPACING} + 9824.17 * \text{SPACING} * \text{SPACING} \quad (9)$$

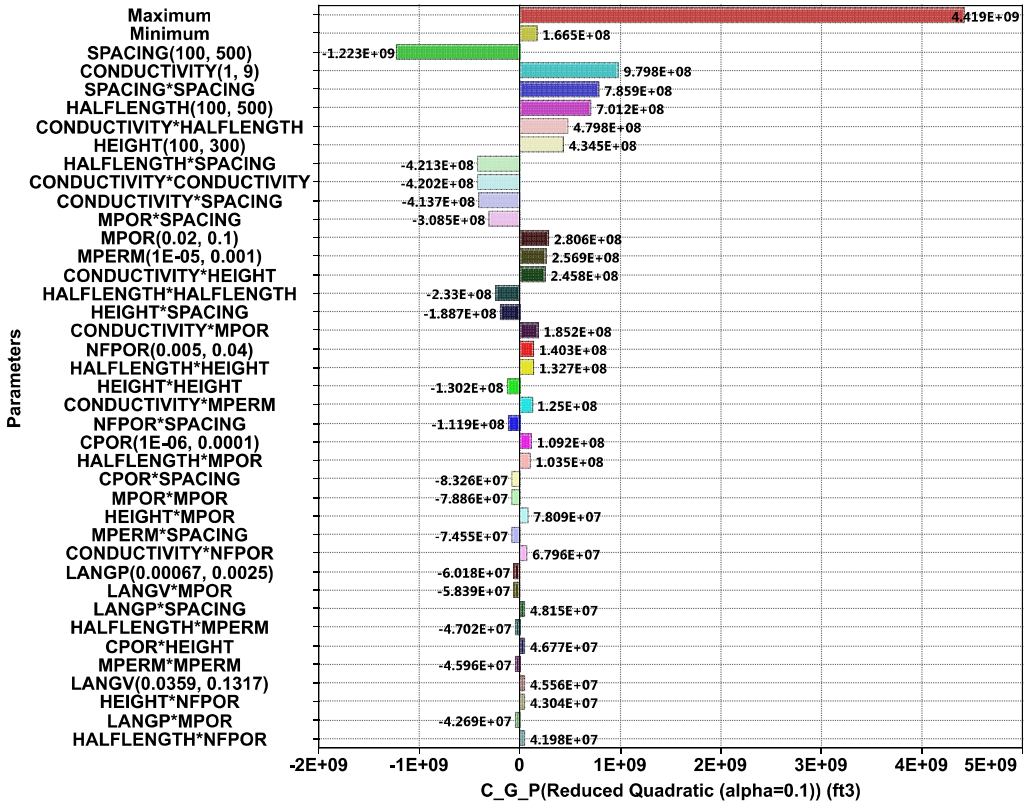

Figure 5.40 Tornado plot of effect estimate for five years cumulative production

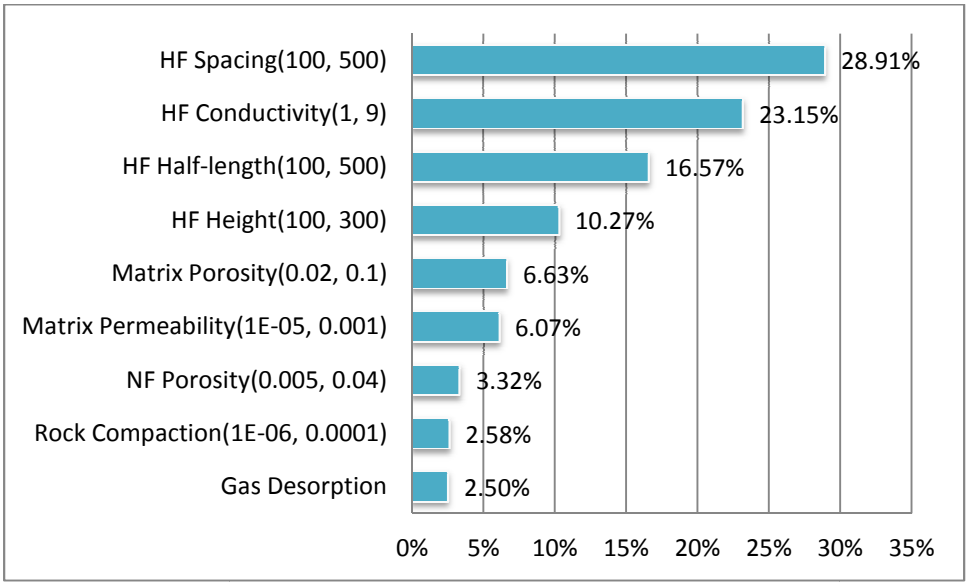

Figure 5.41 Weights of Parameters to Five Years Cumulative Production

5.3.3. Ten Years Production Test. For ten years midterm production analysis, hydraulic fracture properties are still dominating the cumulative production. The weight of hydraulic fracture spacing and conductivity are keeping on decrease. Effect of hydraulic fracture half-length increased to 18.17% (Figure 5.42 and Figure 5.43). Matrix porosity replaces matrix permeability and becomes the most important reservoir parameter.

$$
\begin{aligned}
C_{G_P} = {} & -1.86714 * 10^7 + 8.55309 * 10^7 * \text{CONDUCTIVITY} + 1.60196 * 10^{12} * \text{CPOR} \\
& + 2.60244 * 10^6 * \text{HALFLENGTH} + 2.56749 * 10^6 * \text{HEIGHT} \\
& + 3.60062\text{E} + 10 * \text{LANGP} + 2.43805 * 10^9 * \text{LANGV} + 2.1669 * 10^{11} \\
& * \text{MPERM} + 4.01022 * 10^9 * \text{MPOR} + 7.15161 * 10^9 * \text{NFPOR} \\
& - 2.86895 * 10^6 * \text{SPACING} - 2.10824 * 10^7 * \text{CONDUCTIVITY} \\
& * \text{CONDUCTIVITY} + 1.342 * 10^{11} * \text{CONDUCTIVITY} * \text{CPOR} + 499528 \\
& * \text{CONDUCTIVITY} * \text{HALFLENGTH} + 516045 * \text{CONDUCTIVITY} \\
& * \text{HEIGHT} - 9.00939 * 10^9 * \text{CONDUCTIVITY} * \text{LANGP} + 2.36644\text{E} \\
& + 08 * \text{CONDUCTIVITY} * \text{LANGV} + 7.25419 * 10^{10} * \text{CONDUCTIVITY} \\
& * \text{MPERM} + 8.1483 * 10^8 * \text{CONDUCTIVITY} * \text{MPOR} + 1.64337 * 10^9 \\
& * \text{CONDUCTIVITY} * \text{NFPOR} - 290987 * \text{CONDUCTIVITY} * \text{SPACING} \\
& + 5.71924 * 10^9 * \text{CPOR} * \text{HALFLENGTH} + 1.08014 * 10^{15} * \text{CPOR} \\
& * \text{MPERM} - 8.31537 * 10^9 * \text{CPOR} * \text{SPACING} - 3439.65 \\
& * \text{HALFLENGTH} * \text{HALFLENGTH} + 5252.13 * \text{HALFLENGTH} * \text{HEIGHT} \\
& - 2.10847 * 10^8 * \text{HALFLENGTH} * \text{LANGP} + 2.9585 * 10^8 \\
& * \text{HALFLENGTH} * \text{MPERM} + 1.58147 * 10^7 * \text{HALFLENGTH} * \text{MPOR} \\
& + 1.02882 * 10^7 * \text{HALFLENGTH} * \text{NFPOR} - 8126.64 * \text{HALFLENGTH} \\
& * \text{SPACING} - 6737.99 * \text{HEIGHT} * \text{HEIGHT} - 5.02348 * 10^8 * \text{HEIGHT} \\
& * \text{LANGP} + 2.03773 * 10^7 * \text{HEIGHT} * \text{MPOR} + 1.5689 * 10^7 * \text{HEIGHT} \\
& * \text{NFPOR} - 5325.07 * \text{HEIGHT} * \text{SPACING} + 4.55818 * 10^{13} * \text{LANGP} \\
& * \text{LANGP} + 7.58246 * 10^{11} * \text{LANGP} * \text{MPOR} - 1.76067 * 10^{12} \\
& * \text{LANGP} * \text{NFPOR} - 2.95685 * 10^{10} * \text{LANGV} * \text{NFPOR} - 5.35848 \\
& * 10^6 * \text{LANGV} * \text{SPACING} - 2.49924 * 10^{14} * \text{MPERM} * \text{MPERM} \\
& + 1.8074 * 10^{12} * \text{MPERM} * \text{MPOR} - 5.97373 * 10^8 * \text{MPERM} \\
& * \text{SPACING} - 2.29597 * 10^{10} * \text{MPOR} * \text{MPOR} - 4.29664 * 10^{10} \\
& * \text{MPOR} * \text{NFPOR} - 2.7908 * 10^7 * \text{MPOR} * \text{SPACING} - 2.31976 * 10^7 \\
& * \text{NFPOR} * \text{SPACING} + 11659.3 * \text{SPACING} * \text{SPACING} \qquad (10)
\end{aligned}
$$

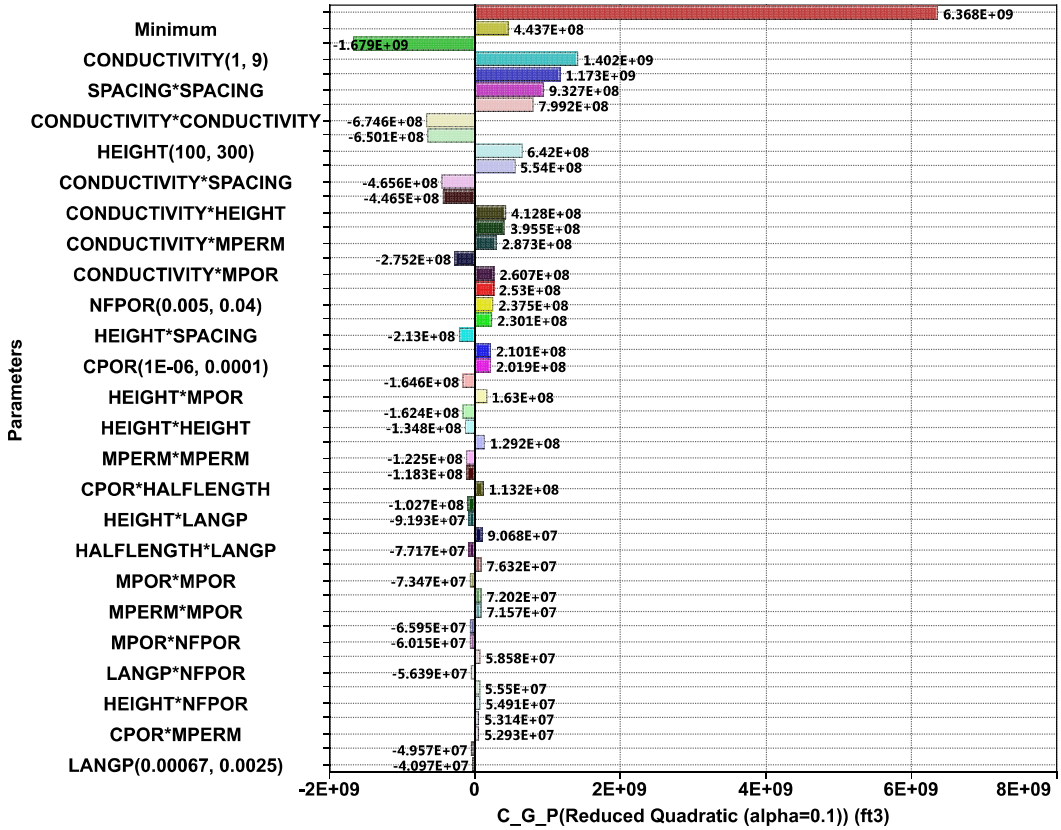

Figure 5.42 Tornado Plot of Effect Estimate for Ten Years Cumulative Production

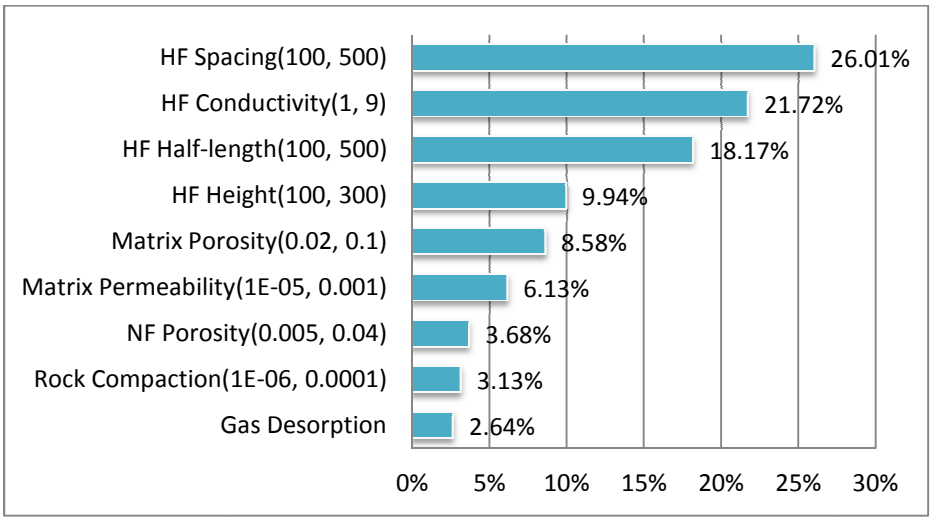

Figure 5.43 Weights of Parameters to Ten Years Cumulative Production

5.3.4. Twenty Years Production Test. For twenty years long term production simulation (Figure 5.44 and Figure 5.45), the effect estimate result is quite different. Hydraulic fracture half-length becomes the most important factor which has a weight of 23.04%. Matrix porosity takes the second place of effect estimate. Fracture height and spacing fail to No. 5 and No. 6 in the ranking.

Overall, for long term production, reservoir parameters become much more significant than ever before, especially for matrix porosity and permeability.

$$
\begin{aligned}
C_{G_P} = {} & 85406.7 - 162.482 * \text{SPACING} + 4028.12 * \text{CONDUCTIVITY} + 53.278 \\
& * \text{HALFLENGTH} + 344.247 * \text{HEIGHT} - 3.43754 * 10^8 * \text{CPOR} \\
& - 2.04685 * 10^7 * \text{LANGP} + 374992 * \text{LANGV} + 2.00989 * 10^7 \\
& * \text{MPERM} - 70757.4 * \text{MPOR} + 1.0169 * 10^6 * \text{NFPOR} + 0.139635 \\
& * \text{SPACING} * \text{SPACING} + 22.4827 * \text{SPACING} * \text{CONDUCTIVITY} \\
& - 0.256237 * \text{SPACING} * \text{HALFLENGTH} + 0.426062 * \text{SPACING} \\
& * \text{HEIGHT} - 650933 * \text{SPACING} * \text{CPOR} + 26232.6 * \text{SPACING} \\
& * \text{LANGP} - 784.399 * \text{SPACING} * \text{LANGV} - 2218.88 * \text{SPACING} \\
& * \text{MPOR} - 1639.29 * \text{SPACING} * \text{NFPOR} - 2571.12 * \text{CONDUCTIVITY} \\
& * \text{CONDUCTIVITY} + 38.7525 * \text{CONDUCTIVITY} * \text{HALFLENGTH} \\
& + 2.75804 * 10^7 * \text{CONDUCTIVITY} * \text{CPOR} + 51634.4 \\
& * \text{CONDUCTIVITY} * \text{LANGV} + 5.0954 * 10^6 * \text{CONDUCTIVITY} \\
& * \text{MPERM} + 105658 * \text{CONDUCTIVITY} * \text{MPOR} + 95748.8 \\
& * \text{CONDUCTIVITY} * \text{NFPOR} - 0.142108 * \text{HALFLENGTH} \\
& * \text{HALFLENGTH} + 1.17193 * 10^6 * \text{HALFLENGTH} * \text{CPOR} + 2804.87 \\
& * \text{HALFLENGTH} * \text{MPOR} + 2021.77 * \text{HALFLENGTH} * \text{NFPOR} \\
& - 1.11206 * \text{HEIGHT} * \text{HEIGHT} + 1.19629 * 10^6 * \text{HEIGHT} * \text{CPOR} \\
& + 1886.33 * \text{HEIGHT} * \text{MPOR} + 2.27798 * 10^9 * \text{CPOR} * \text{MPOR} \\
& + 1.26682 * 10^8 * \text{LANGP} * \text{MPOR} - 2.32313 * 10^6 * \text{LANGV} * \text{MPOR} \\
& + 3.04337 * 10^8 * \text{MPERM} * \text{MPOR} - 8.30986 * 10^6 * \text{MPOR} \\
& * \text{NFPOR} \qquad (11)
\end{aligned}
$$

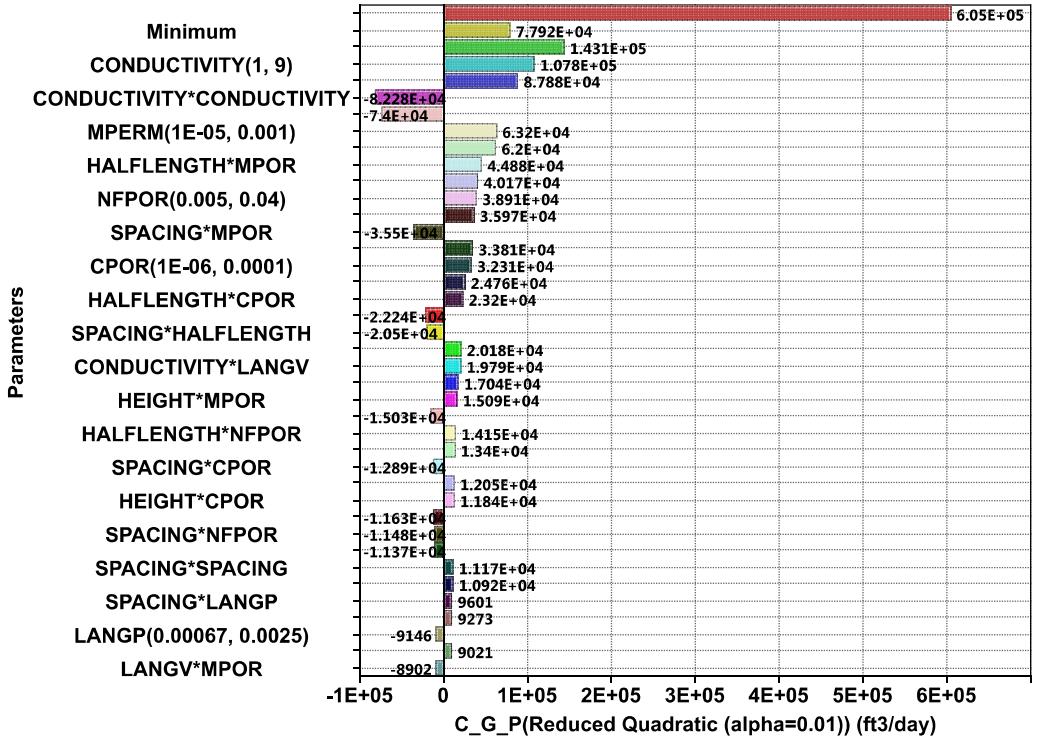

Figure 5.44 Tornado Plot of Effect Estimate for Twenty Years Cumulative Production

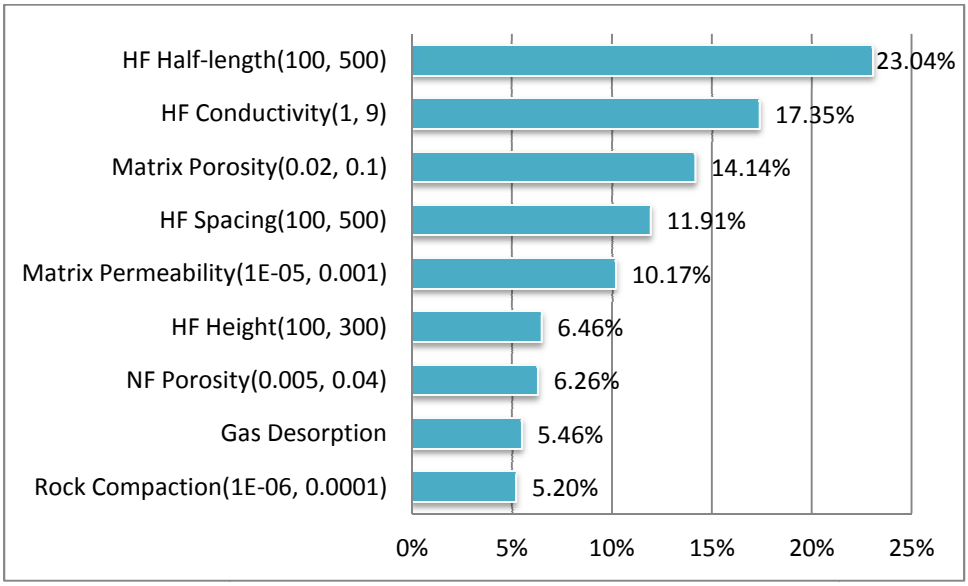

Figure 5.45 Weights of Parameters to Twenty Years Cumulative Production

5.3.5. Summary of Sensitivity Analysis with Different Time Periods. Figure 5.46 gives the summary of sensitivity analysis basing on different time periods. It is clear that the influences of rock compaction, natural fracture porosity, gas desorption, matrix porosity, matrix permeability and hydraulic fracture half-length are increasing with time. On the other hand, effects of hydraulic fracture height, hydraulic fracture conductivity, and hydraulic fracture spacing are decreasing with time.

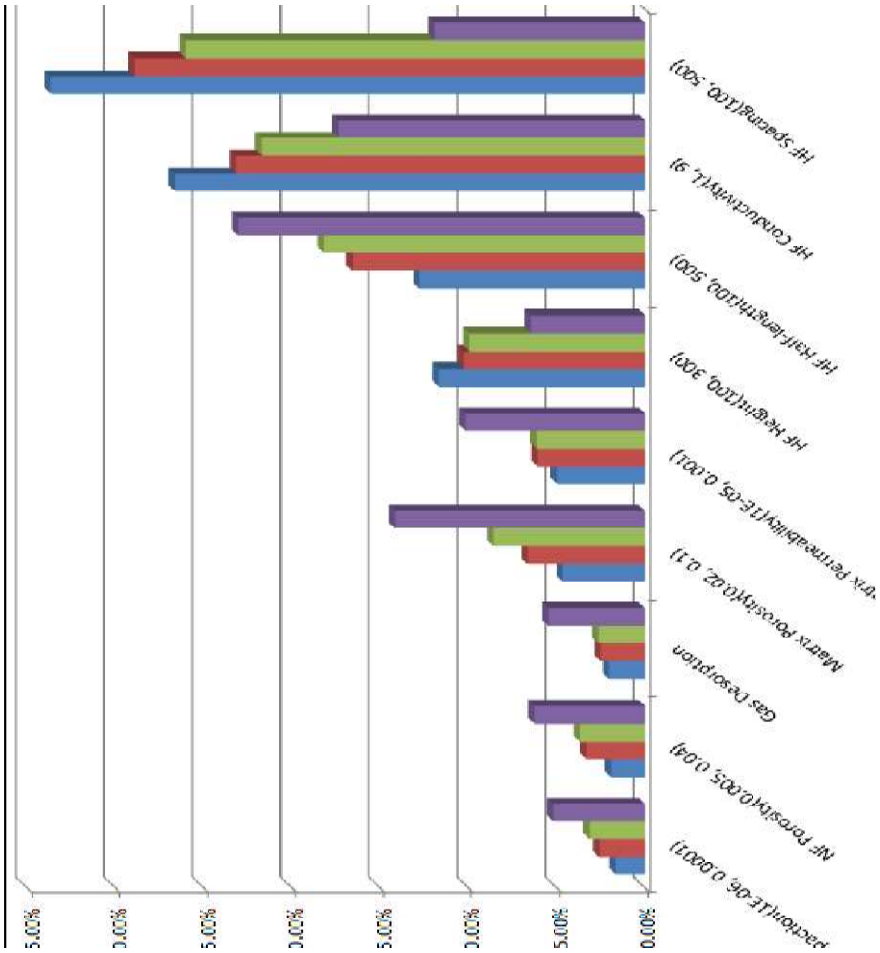

Figure 5.46 Summary of Sensitivity Analysis

6. CONCLUSION

A three dimensional single phase dual-permeability shale gas reservoir model has been built. Three kinds of flow mechanisms (Darcy flow, Non-Darcy flow, and Gas diffusion) as well as gas adsorption and desorption mechanism have been considered in this model. A multi-stage hydraulically fractured horizontal well is located in the middle of the model.

The effect several reservoir parameters and hydraulic fracture parameters to cumulative production have been studied. Reservoir parameters (including matrix permeability, matrix porosity, natural fracture porosity, rock compressibility, and gas desorption) and hydraulic fracture parameters (hydraulic fracture spacing, hydraulic fracture half-length, hydraulic fracture conductivity, and hydraulic fracture height) have been studied separately. Result of these studies can be used to improve the efficiency of history match and help to accurately forecast shale gas production performance.

Hydraulic fracture spacing, half-length, conductivity and height are all significant parameters for production performance, especially for short term production. For long term study, the effect of hydraulic fracture parameters will decrease relatively.

Compared with hydraulic fracture parameters, the influences of reservoir parameters are insignificant in short term production. However, in long term testing, the effect of matrix porosity and permeability become very important to the cumulative production. Natural fracture porosity shows similar trend, but does not have that great effect. Effects of gas desorption and rock compaction, although are increased over time, are remaining in low level for all production analysis.

Influences of reservoir parameters and hydraulic fracture parameters for different time periods were quantified by simulation for 1 yr., 5 yr., 10 yr., and 20 yr. production and the results were analyzed.

BIBLIOGRAPHY

Bumb, A. C., & McKee, C. R. (1988, March 1). Gas-Well Testing in the Presence of Desorption for Coalbed Methane and Devonian Shale. SPE-15227-PA.

Carlson, E.S. and Mercer, J.C. 1991. Devonian Shale Gas Production: Mechanisms and Simple Models. JPT (April 1991): 476–482. SPE-19311-PA.

Cipolla, C. L., Lolon, E. P., Erdle, J.C., and Rubin, B. 2010. Reservoir Modeling in Shale-Gas Reservoirs. SPEREE, August, 638-653. SPE-125530-PA.

Daniels, F. and Alberty, R.A.: Physical Chemistry, John Wiley & Sons, Inc., New York (1957) 524.

Dehghanpour, H., & Shirdel, M. (2011, January 1). A Triple Porosity Model for Shale Gas Reservoirs. SPE-149501-MS.

Du, C.M., Zhang, X., Lang, Z., Gu, H., Hay, B., Tushingham, K. and Ma, Y.Z. 2010. Modeling Hydraulic Fracturing Induced Fracture Networks in Shale Gas Reservoirs as a Dual Porosity System. Paper SPE 132180.

Freeman, C. M. (2010, January 1). A Numerical Study of Microscale Flow Behavior in Tight Gas and Shale Gas. SPE-141125-STU.

Fisher, M.K., Heinze, J.R., Harris, C.D., Wright, C.A., and Dunn, K.P. 2004. Optimizing Horizontal Completion Techniques in the Barnett Shale using Microseismic Fracture Mapping. Paper SPE 90051 presented at the SPE Annual Technical Conference and Exhibition held in Houston, Texas, USA, 26-29 September.

F. JAVADPOUR, D. FISHER, M. UNSWORTH. 2007. Nanoscale Gas Flow in Shale Gas Sediments. Journal of Canadian Petroleum Technology. October 2007, Volume 46, No. 10.

H. Huang and J. Ayoub, Applicability of the Forchheimer Equation for Non-Darcy Flow in Porous Media. September, 2006, SPE 102715.

Julia F. W. Gale, Robert M. Reed, and Jon Holder, “Natural fractures in the Barnett Shale and their importance for hydraulic fracture treatments” AAPG Bulletin, v. 91, no. 4 (April 2007), pp. 603–622, 2007.

Li, J., Du, C.M., and Zhang, Xu. 2011. Critical Evaluation of Shale Gas Reservoir Simulation Approaches: Single Porosity and Dual-Porosity Modeling. Paper SPE 141756.

Michael D. Max, Arthur H. Johnson, William P. Dillon, 2006. Economic Geology of Natural Gas Hydrate. ISBN-1402039727.

Moridis, G.J., Blasingame, T. A., and Freeman, C. M. 2010. Analysis of Mechanisms of Flow in Fractured Tight-Gas and Shale-Gas Reservoirs. SPE 139250.

Pereira, C. A., Kazemi, H., & Ozkan, E. (2006, October 1). Combined Effect of Non-Darcy Flow and Formation Damage on Gas Well Performance of Dual-Porosity and Dual-Permeability Reservoirs. Society of Petroleum Engineers. doi:10.2118/90623-PA.

Pruess, K., C. Oldenburg, and G.Moridis, 1999, TOUGH2 User's Guide – Version 2.0, Lawrence Berkeley Laboratory Report LBL-43134, Berkeley, CA.

Pruess, K. (1985, February 1). A Practical Method for Modeling Fluid and Heat Flow in Fractured Porous Media. Society of Petroleum Engineers. doi:10.2118/10509-PA

Rahmanian, M. R., Solano, N., & Aguilera, R. (2010, January 1). Storage And Output Flow From Shale And Tight Gas Reservoirs. SPE-167124-MS.

Swami, V., Clarkson, C. R., & Settari, A. (2012, January 1). Non-Darcy Flow in Shale Nanopores: Do We Have a Final Answer? SPE-162665-MS.

Warpinski, N., Kramm, R. C., Heinze, J. R., & Waltman, C. K. (2005, January 1). Comparison of Single-and Dual-Array Microseismic Mapping Techniques in the Barnett Shale. SPE 95568-MS.

Wei Yu, Kamy Sepehrnoori, 2013. Simulation of Gas Desorption and Geomechanics Effects for Unconventional Gas Reservoirs. SPE-165377.

Wu, Y.-S., & Pruess, K. (1988, February 1). A Multiple-Porosity Method for Simulation of Naturally Fractured Petroleum Reservoirs. Society of Petroleum Engineers. doi:10.2118/15129-PA.

Yan, B., Wang, Y., and Killough, J. 2013. Beyond Dual-Porosity Modeling for the Simulation of Complex Flow Mechanisms in Shale Reservoirs. SPE 163651.

Zhang, X., Du, C., Deimbacher, F., Crick M., and Harikesavanallur, A. 2009. Sensitivity Studies of Horizontal Wells with Hydraulic Fractures in Shale Gas Reservoirs. IPTC 13338.

VITA

Jiaqi Wang was born in 1990. He received his Bachelor's degree in Petroleum Engineering from China University of Geosciences, Beijing (2012). He started his Master's degree in Petroleum Engineering at Missouri University of Science and Technology which was awarded in May of 2014.